

Energy harvesting from ear canal during speaking: feasibility study and finite element simulation

Mohammadreza Salemi, MSc student, Department of Mechanical Engineering, Yazd University, P.O. Box 89195-9741, Yazd, Iran, Tel.: +983536247689, Mobile: +989133585371, salemi@stu.yazd.ac.ir

Mohammad Mahdi Jalili*, Associate professor, Department of Mechanical Engineering, Yazd University, P.O. Box 89195-9741, Yazd, Iran, Tel.: +983531233893, Mobile: +989133532247, jalili@yazd.ac.ir

Mohammad Jafari, Assistant professor, Department of Mechanical Engineering, Yazd University, P.O. Box 89195-9741, Yazd, Iran, Tel.: +9831232565, Mobile: +989137741838, mjafari@yazd.ac.ir

Mohammad Hadi Honarvar, Assistant professor, Department of Mechanical Engineering, Yazd University, P.O. Box 89195-9741, Yazd, Iran, Tel.: +9831232506, Mobile: +989127981207, hadihonarvar@yazd.ac.ir

Abstract

Ear canal deformation caused by jaw joint movement is simulated in this paper and introduced as a candidate source of power to supply hearing aids devices power. The ear mold is prepared and the CT-Scan is performed using this mold in both open and close positions of the mouth. The ear canal model is created with Mimix, 3matic and Catia softwares. The mandible motion in cases of discussion, text reading, poem reading, greeting and speaking loudly is captured by opti-track camera and processed in Matlab software. Ear canal model and mandible path are imported to Abaqus finite element analysis software. Using the finite element model the output voltage of piezoelectric for each case of talking is calculated. Required electrical circuit to convert generated voltage from AC to DC is modeled in Matlab simulink and output power is determined. The results show that this module could supply a low power hearing aid for about 14 hours with considering individual talking activity per day. Also, with increasing the human age, the amount of output voltage from the piezoelectric harvesting device increases.

Keywords: Ear canal, Energy harvesting, Finite element model, Piezoelectric, Speaking.

1 Introduction

Reducing power usage of in ear devices increases probability of their energy supply with energy harvesting methods instead of using batteries [1]. Energy can be harvested from environment or human body. Using environment sources like solar, radiant and acoustic energies for this purpose is not rational because the environment is unstable [2-4]. Human body is an abundant source of power and in this case has more potential than the environment. Energy can be harvested from upper limb motion such as full bicep curls and arm lift [5, 6], walking which has many different method such as using heel strikes [7, 8], knee movement [9], leg movement [10]. Body heat [11] specially in neck [12] and head [13], air flow during breathing [14], blood pressure [15], heart beat [16], head movement [17], muscle force [18], endocochlear potential (electrochemical energy) [19] are other examples of energy sources in human body. Most of these sources of energy have high potential for power supplying in ear devices due to proximity to ear. However, these sources are too limited or unsuitable for hearing devices.

Due to proximity between power supply and in ear device , ear canal dynamic motion has been recently suggested as a human body source of energy. Compared to other methods, using piezoelectric materials are more compatible with in ear application [20]. Piezoelectric materials generate an electrical charge when subjected to a mechanical stress [21]. The type of piezoelectric substantially influences harvester performance and user convenience. A flexible piezo material should be chosen for in ear devices to withstand extensive strain in the ear. This material should also be biocompatible, therefore polyvinylidene fluoride (PVDF), piezoelectric fiber composite, piezoelectric fine wires and piezoelectric meta materials are usually used for this purpose [22-24].

Some researchers have been focused on harvesting energy from ear canal deformation. Delnavaz and Voix [25] investigated the effect of jaw joint movement on the change in the volume of the ear canal for a group of 12 people between 23 to 60 years old. This change of volume was interpreted as a change of water level in a vertical tube to measure its energy. They predict that this power can supply fully or at least partially the required power of hearing devices. Furthermore, they [26] developed a finite element model to estimate the energy harvesting capability of the piezoelectric layer. A hydroelectromagnetic energy harvester and a flexible piezoelectric generator were created by Delnavaz and Voix [20] to experimentally study the possibility of using energy harvesting from ear canal dynamic motion as a source of power to replace the use of batteries for

in-ear devices. Using ear canal point clouds, Carioly et al. investigated the bending and compressive movements of the ear canal to select an appropriate deformation mode for harvesting energy from the ear canal dynamic motion [27]. A bulk piezoelectric ceramic was integrated by Delnavaz and Voix [28] onto a flexible platform for energy harvesting from the human body pressing force. They investigated the von mises yield criterion by using finite element analysis to make sure that the PZT beam tolerates the applied stresses. Carioli et al. [29] calculated the PVDF output voltage due to jaw movements by applying Winkler-Bach theory and the piezoelectric constitutive equation for two extreme jaw positions. Wang et al. [30] proposed a liquid-filled earplug energy harvester which transfers energy outside the ear canal to a generator and composed of a hydraulic amplifier, two hydraulic cylinders that actuate a bistable resonator to raise the source frequency while driving an amplified piezoelectric transducer to generate electricity.

Charging the battery of ear devices is one of the problems of their users due to the forgetfulness of the user and the lack of access to a suitable charging source in any place. Due to the reduction of energy consumption of these devices by increasing their efficiency, the use of energy harvesting methods to provide part of the energy consumption of these devices can reduce the problem of their continuous charging. Therefore, in this article, the possibility of harvesting energy from the ear canal to supply energy of in-ear devices such as hearing aids and headphones is investigated.

Briefly, following three main gaps can be addressed in the literature:

1. Despite the existing valuable works in the available literature, no research has been done to investigate the harvesting of energy from ear canal during speaking, by considering a full model of the ear canal cartilage, ear mold, piezoelectric layer and condyle of mandible.

2. Some of the studies that investigate the effects of jaw movement cycle on energy production during the speaking, used simple moving of a solid sphere to model the mandibular condyle motion.

3. Very few studies have investigated the effects of ear canal and speaking parameters on energy harvesting of the ear plugin. In all of them, experimental setup has been used for parametric investigation. Using experimental methods for determining the effects of different parameters on energy harvesting from ear canal is expensive and very time-consuming. Therefore, this study is novel in terms of the following aspects:

1. In the current work, a full finite element model for in ear energy harvesting

containing the model of ear canal cartilage, ear mold, piezoelectric plugin and mandibular condyle is developed using Abaqus software.

2. To determine ear canal excitation, actual motion of the mandible during different type of speaking is determined using opti-track camera. These data are imported in finite element simulation to determine the generated power by the system during the speaking.

3. Using the finite element model developed in this research, effects of different parameter like PVDF orientation, cartilage and ear mold stiffness, coefficient of friction between condyle of the mandible and soft tissue and different talking type on the power generated by the system are investigated.

2 Materials and methods

In order to study the energy harvesting from ear canal during speaking, a finite element model of the ear canal including piezoelectric layer is developed. To begin, geometrical models of the ear canal in both open and close positions of the mouth are developed, based on data obtained from CT-scan. Afterward, homogeneous mechanical properties of different parts of model are used to simulate the behavior of ear canal due to mandible motion during speaking. Finally, using a full wave rectifier bridge circuit to convert AC voltage generated by piezoelectric layer to DC voltage, the electric power harvested by piezoelectric is calculated. The experimental protocol of this research, was approved by the ethics committee at the vice chancellery for research and technology affairs of the Yazd university with letter No.: 12/SAD/1478.

2.1 Modeling

A comprehensive model of ear canal including piezoelectric layer, jaw joint movement and electric circuit for capacitor charging will be presented to simulate the possibility of energy harvesting from ear canal motion. For finite element modeling of ear canal, the ear canal geometry should be extracted. Different methods can be used to obtain ear canal geometry. One of them is to use silicon ear mold and then scan it by 3D laser coordinate measuring machine [31], the other one is using computer assisted tomographic scanner (CT-Scan) [32]. Other methods include magnetic resonance scanner [33] and ear canal laser scanning [34].

In this paper ear canal geometry was obtained using CT-Scan method. First of all ear mold

was fabricated in open mouth position as shown Fig. 1. For this purpose, a mouth prop was used between front teeth to keep the mouth in an open position up to a maximum of 25 mm. Afterwards, room temperature vulcanizing (RTV) silicon was injected in to the ear canal and after 10 minutes earmold was removed.

CT-Scan was performed using this mold in both open and close position of the mouth. It must be considered that the mouth prop also be used for open positions. Three images of the ear canal cross sections obtained by CT-Scan are shown in Fig. 2. In the following, the images of ear canal cross sections were imported to Materialise Mimix software and converted to point-cloud. The point cloud results were imported to Materialise 3matic software for surface modification. The results were imported to Catia software and different parts; soft tissue, Ear mold, part of temporal and condyle of mandible were created. Then these parts were imported to finite element software to analyze. The workflow for generating the ear canal geometry is shown in Fig. 3.

As shown in Fig. 4, for modeling the piezoelectric layer, a part of the plugin surface with 110 micrometer thickness is defined as piezoelectric layer.

2.2 Mandible motion

To determine ear canal excitation, mandible motion during speaking should be determined. Mandible motion can be captured by electromagnetic sensors, acoustic sensors or photogrammetric systems. In this paper opti-track camera was used for this purpose. The camera has a surface of light sensitive diodes and coordinates are recorded by sending and receiving light reflections by sensors. As illustrated in Fig. 5, one of the markers is connected to the chin. Since the head movement changes this marker position and fixing of the head was impossible, two markers were located on forehead and one marker was located on temporal bone near auricle to define new coordinate system which connected to the head.

Data collection was performed in seven cases: closed mouth, open mouth, discussion, reading a text, reading a poem, greeting and speaking out loud. For the closed mouth position, the mouth was closed for 5 second to obtain this position. Also, for the open mouth position, the mouth was opened for 5 second to obtain this position. This process is shown in Fig. 5.

The acquired data were imported to Matlab software. Then, chin marker position was

transferred to head coordinate system and mouth closing percent was achieved. The results are presented in Fig. 6. Because of great variation of the mandible motion amplitude, utilization of these data as a source of ear canal excitation in Abaqus software increases the simulation time. Therefore these values must be simplified before simulating. For this purpose fast fourier transform (FFT) was used to obtain the main frequencies of the excitation signal. Because of frequencies of mandible motion does not exceed 2 hertz in accordance with FFT results, so all frequencies below 2 hertz were averaged by weighted mean method by considering amplitude of each frequency as the weight.

Using this method, the equal frequencies of discussion, text reading, poem reading, greeting and speaking loudly are calculated 0.126, 0.527, 0.363, 0.928, 1.281 hz, respectively. According these frequencices, equal digrams for mouth closing during the time are presented in Fig. 6.

2.3 Simulation

In this paper, Abaqus finite element analysis software is used to investigate the characteristics and performance of the energy harvesting module. The model is composed of four geometrical domains: cartilage, earmold, part of temporal bone and condyle of the mandible as shown in Fig. 7.

2.3.1 Materials properties

In this paper, cartilage and earmold are represented by a linear elastic materials whose their mechanical properties are presented in Table1. All values are from the manufacturer's technical manual.

The average stiffness of cortical and spongy bones are 18.6 and 10.8 GPa respectively [38]. Because of the fact that this values are much more than stiffness of cartilage and earmold, they considered as rigid bodies. In finite element simulation, the relation between the PVDF strain and charge is considered as Eq. (1):

$$\begin{aligned} S &= S_e T + d^T E \\ D &= dT + \varepsilon E \end{aligned} \tag{1}$$

where T, S, E and D are the reordered components of stress, strain, electric field and electric displacement, respectively. Also, ε is electric permittivity, S_E is the compliance matrix and d is the coupling matrix. Numerical values for the material specific of the PVDF are defined in Eqs. (2) and (3) [39]:

$$d = \begin{bmatrix} 0 & 0 & 0 & 0 & -27 & 0 \\ 0 & 0 & 0 & -23 & 0 & 0 \\ 23 & 23 & -33 & 0 & 0 & 0 \end{bmatrix} \times 10^{-12} \text{CN}^{-1} \quad (2)$$

$$S_E = \begin{bmatrix} 39.5 & -10.2 & -25.4 & 0 & 0 & 0 \\ -10.2 & 42 & -19.5 & 0 & 0 & 0 \\ -25.4 & -19.5 & 99.9 & 0 & 0 & 0 \\ 0 & 0 & 0 & 1.82 & 0 & 0 \\ 0 & 0 & 0 & 0 & 1.69 & 0 \\ 0 & 0 & 0 & 0 & 0 & 1.43 \end{bmatrix} \times 10^{-12} \text{m}^2 \text{N}^{-1} \quad (3)$$

Also, the PVDF permittivity is in accordance with relation (4):

$$\varepsilon = \begin{bmatrix} 110 & 0 & 0 \\ 0 & 110 & 0 \\ 0 & 0 & 110 \end{bmatrix} \times 10^{-12} \text{Fm}^{-1} \quad (4)$$

The young's modulus, poisson's ratio and density of the PVDF are 3 GPa, $1780 \frac{\text{kg}}{\text{m}^3}$ and 0.35 respectively.

2.3.2 Boundary conditions and constraints

The required boundary conditions for modeling the energy harvesting is determined from ear canal dynamic behavior. For easier identification of the surfaces that are in contact with each other, they are shown with the same letters in Fig. 8. The ear mold surface and ear surface are tied together because ear mold is fitted in ear canal. These surfaces are marked with the letter C in the Fig. 8. Head of ear mold which is in contact with ear canal bony section, has a rough friction with

temporal bone which prevents sliding of surfaces. These surfaces are marked with the letter D in the Fig. 8. Outer surfaces of temporal and inner surface of cartilage which are adjacent to each other are tied together as shown with A letter. Sliding friction is defined between condyle and cartilage with coefficient of friction of 0.36 that these surfaces are indicated with B letter. [40]. Electric potential is set to zero on piezoelectric outer surface and equal all over inner surface.

2.3.3 Mesh

Because of the complexity of geometry of ear canal/piezoelectric system, tetrahedron element type is used for meshing the model. Moreover, first order elements are selected to reduce computing time. The models were discretized by tetrahedron elements (C3D4I) with an approximate size of 0.5 . A mesh convergence study revealed that using a finer mesh did not change the results significantly. Abaqus implicit solver was used to compute the voltage of the model. Discretized model has been shown in Fig. 9.

3 Results

To estimate the electric potential generated by piezoelectric during speaking, finite element analysis is performed in one full mouth opening and closing cycle with cartilage middle stiffness. We consider the piezoelectric orientation that the main direction is perpendicular to the piezoelectric surface. The obtained result from finite element simulation for different states, greeting, speaking loudly, reading poem, reading text, and discussion are shown in Fig. 10. As can be seen in this figure, the frequency of the generated voltage varies depending on the type of the speech and is equal to the speaking frequency.

Piezoelectric materials only generate voltage due to the change of the applied force. Under constant force, the output voltage quickly reaches to zero because of high internal resistance. Because of the fact that it's not possible to consider this matter in the simulation, the output voltage does not change and fluctuates around a constant value. Therefore, only different voltage generated by the simulation is reliable which are 2.25, 3.2, 1.75, 2.55 and 2.45 volts for the states of greeting, speaking loudly, reading poem, reading text, and discussion respectively.

Ear canal deformation divided into radial compression and bending in which both of them

leads to deform piezo material perpendicular to its surface. PVDF could take three orientation in this direction as shown in Fig. 11. Output voltage for each orientation is obtained for cartilage middle stiffness during full chewing cycle as shown in Fig. 12. According to the results, among these orientations longitudinal direction exhibits maximum output voltage which reaches 4.030 volts.

The piezoelectric plugin is usually subjected to oscillating loads. Therefore, research about its fatigue behavior is very important. Fig. 13 illustrates distribution of the von mises stress in piezoelectric plugin. As shown in this figure the stress starts from 0.09 MPa and increases in the first and second bends due to the greater effect of bending loading than the compression. According to Fig. 13, the equivalent stress reaches to 23.5 MPa in the first bend, which is less than the piezoelectric yield stress. Therefore the maximum stress is in the elastic range. Due to the intermittent movement of the jaw, the oscillating change of stress is applied to the piezoelectric. Hence, the safety factor of this material under fatigue in the oscillating state with the maximum frequency is studied in this research. For this reason, full opening and closing mouth is considered. Using the soderberg criterion and according to Eq. (5) and setting the yield strength equal to 51 MPa [42], the safety factor of 1.5 is obtained, which is acceptable.

$$\frac{\sigma_a}{S_e} + \frac{\sigma_m}{S_y} = \frac{1}{n} \quad (5)$$

It must be considered that in in real situations, the mouth is not fully opened and frequency is also below chewing frequency. Therefore, the considered situation is the most critical situation and hence fatigue will not happen in other situations.

4 Discussion

The simulation results of the piezo-earpiece model presented in the previous sections depend on mechanical properties of its componenets. The stiffness of cartilage and friction coefficient between condyle and cartilage vary among individuals and depends on the age of the people and the force between muscle and bone, respectively. Ear mold material could also change.

With increase in the human age, the cartilage stiffness increases. For age range of 59 ± 10 years, cartilage stiffness varies in the range of 1.66 ± 0.63 MPa. Fig. 14 shows the effect of different cartilage stiffness, $E=1.03, 1.66, 2.29$ Mpa, on the piezoelectric strain. According to this figure,

with increase in the cartilage stiffness the strain in the piezoelectric increases.

Effect of cartilage stiffness due to human age on output voltage in piezoelectric longitudinal direction is presented in Fig. 15. As shown in this figure, the output voltage increases to 5 volts with increase the human age to 69 years. Also this figure shows that with age decreasing to 49 years, the output voltage decrease to 2.75 volts. Also, as illustrated in Figs. 14 and 15 cartilage stiffness increasing cause more strain in piezoelectric and consequently more electric potential.

Ear mold stiffness can affect the output voltage by changing the piezoelectric strain. Fig. 16 illustrate the distribution of strain within the piezoelectric for different earmold stiffness, $E=1.66, 1.25, 0.83$ Mpa. As shown in Fig. 16, decreasing the ear mold stiffness increases the piezoelectric strain.

Increasing the stiffness of the ear mold to the extent that it does not cause discomfort to the person and decreasing it to the extent that it does not come out of ear canal is possible. Piezoelectric and ear mold withstand ear canal stress together, softer ear mold withstand less stress portion and impose more stress on piezoelectric. Effect of ear mold stiffness on output voltage in piezoelectric longitudinal direction is shown in Fig. 17. According to the results, with increase the ear mold stiffness, the maximum output voltage decreases to 2.676 volts which shows 36.5% reduction of output voltage compared to output voltage with soft ear mold. As shown in Table 2, new RTV silicone rubbers with lower modulus of elasticity have been produced. Using these RTVs can generate more electrical power than the results presented in Fig.14.

Coefficient of static friction between bone and muscle tissue varies from 0.29 to 0.36 and change from one person to another. Also, kinetic friction coefficient is fluctuating around a constant level which is slightly less than the static friction coefficient. Fig. 18 depicts the piezoelectric strain with different coefficient of friction between condyle of the mandible and soft tissue. As can be seen in Fig. 18, piezoelectric strain is proportional with coefficient of friction between condyle of the mandible and soft tissue and its increase causes more strain and consequently more electric potential.

Effect of coefficient of static friction on piezoelectric output voltage in longitudinal direction is investigated in Fig. 19. As shown in this figure, reduction of coefficient of static friction, reduces the output voltage.

To investigate the possibility of energy supply of the ear devices by energy harvesting of

the ear canal, the electric power generated by piezoelectric should be determined. For calculating the generated power, first of all the simulated voltage must be converted to the actual voltage according to actual mandible movement. Then this voltage should be converted to DC voltage for charging the ear device battery. Because the model is linear, the output voltage is proportional to the mandible movement. For this purpose, by averaging mandible closing percent during the simulation, mandible average position is achieved and considered as mandible position at zero output voltage. Then maximum output voltage corresponds to the maximum mouth closing percent and actual output voltage is achieved. The results are shown in Fig. 20.

This variable voltage is not usable in electronic devices and must be converted to DC voltage. In this research, a full wave rectifier bridge and a 24 micro farad current smoothing capacitor is used for this reason as presented in Fig. 21.

Required circuit is modeled in Matlab simulink as shown in Fig. 21 and capacitor charging time is achieved. By knowing the charging time of the capacitor, the impedance of the capacitor can be calculated by Eq. (6),

$$Z = X_c = \frac{1}{2\pi fC} \quad (6)$$

which f is capacitor charging frequency and C is the capacitance of capacitor. Then, electrical energy harvested from ear canal motion can be calculated by Eq. (7),

$$E = \frac{1}{Z} \times \int_{t_0}^t V_{(t)}^2 dt \quad (7)$$

which Z is the amount of impedance that the signal drives. It is the capacitor impedance in this case [43]. Also, the average output power can be calculated using Eq. (8).

$$P = \frac{E}{t} \quad (8)$$

Using Eq. (8), the average output power for discussion, text reading, poem reading, greeting and speaking loudly cases is calculated that is equal to 1.14, 0.17, 1.6, 3.89 and 2.75 micro watts respectively. It should be noted that some of this power is wasted by the circuit elements such as wires and diodes.

By experimental observation about the person studied in this research during one week, the average times spent for each case of speaking are extracted. Using these results the harvested energy by piezoelectric for each case and total generated energy are calculated. The results are presented in Table 3. The total energy can be generated by the presented model is 13.8 mJ.

Considering that the power consumption of ear device is about 0.964 milliwatts [1], the designed ear plugin can supply its energy for about 14 hours in a day.

5 Conclusion

In this paper an ear plugin consist of a soft ear mold wrapped in a flexible layer of PVDF for energy harvesting from the ear canal dynamic motion was investigated. Finite element modeling was used to simulate the mechanical deformation and electrical potential generation capability of the device. For the electromechanical modeling, the ear mold was made and CT-Scan was performed using this mold. The model was created by Mimix, 3matic and Catia softwares and the mandible path was obtained by data collection and Matlab processing. The simulating results were achieved through Abaqus software. Also output voltage for discussion, text reading, poem reading, greeting and speaking loudly cases was calculated. Required circuit for converting AC voltage to DC voltage was modeled in Matlab software and output power for discussion, text reading, poem reading, greeting and speaking loudly was calculated and average output power was achieved for each cases. Based on the results obtained in this paper, the following conclusions can be made:

1. With increasing the human age, the amount of output voltage from the piezoelectric harvesting device increases. This result is important because with increasing age, the probability of using hearing aids increases.
2. Reduction of static coefficient of friction between soft tissue and condyle of the mandible, reduces the output voltage.
3. Maximum output voltage increase with softer silicon ear mold.
4. To achieve maximum power, piezoelectric orientation must be chosen so that the main piezoelectric direction is perpendicular to the ear canal surface.
5. The designed ear plugin could supply energy of in ear devices for about 14 hours in a day.

The model examined in this research is related to a specific ear canal and its associated bone structure. The amount of energy that can be harvested from the ear canal in different people with different ages can be investigated in the continuation of this research. Also, investigation of

the amount of energy production in different speaking states, in addition to the cases discussed in this article, can also be done in future researches.

Design and construction of a plugin with a piezoelectric layer that can be placed in the ear canal along with a current rectifier circuit for charging the battery are the steps required to build this device. It should be noted that this device should be small and of suitable weight to satisfy the users.

Declaration of Competing Interest

The authors declare that they have no known competing financial interests or personal relationships that could have appeared to influence the work reported in this paper.

Funding

The authors received no financial support for the research, authorship, and/or publication of this paper.

Ethical approval

The experimental protocol of this research, was approved by the ethics committee at the vice chancellery for research and technology affairs of the Yazd university with letter No.: 12/SAD/1478.

References

- [1] Qiao, P., Corporaal, H. and Lindwer, M. “A 0.964 mw digital hearing aid system”, *2011 Design, Automation & Test in Europe*, Grenoble, France, pp. 1–4 (2011).
<https://doi.org/10.1109/DATE.2011.5763297>
- [2] de Sa, M.H., Pinto, A.M.F.R. and Oliveira, V.B. “Passive direct methanol fuel cells as a sustainable alternative to batteries in hearing aid devices - An overview”, *Int. J. Hydrogen Energy*, **47**(37), pp. 16552-16567 (2022).
<https://doi.org/10.1016/j.ijhydene.2022.03.146>.
- [3] Marian, V., Allard, B., Vollaire, C., et al. “Strategy for microwave energy harvesting from ambient field or a feeding source”, *IEEE Trans. Power Electron.*, **27**(11), pp. 4481–4491 (2012).
<https://doi.org/10.1109/TPEL.2012.2185249>.
- [4] Karimzadeh, A., Roohi, R. and Akbari, M. “Piezoelectric wind energy harvesting from vortexinduced vibrations of an elastic beam”, *Sci. Iran., Trans. B*, **30**(1), pp. 4726–4730 (2023).
<https://doi.org/10.24200/sci.2022.59718.6393>.
- [5] Rathod, P.B., Makandar, N., Suguresh, K., et al. “Analysis of Energy Harvesting from Human Motion” *2022 IEEE North Karnataka Subsection Flagship International Conference*, Vijaypur, India, pp.12-18 (2022).
<https://doi.org/10.1109/NKCon56289.2022.10126597>.
- [6] Gao, S., He, T., Ao, H., et al. “Investigation of self-oscillation piezoelectric energy harvesting mechanics for lower-limb motion”, *2021 IEEE 20th International Conference on Micro and Nanotechnology for Power Generation and Energy Conversion Applications*, Exeter, United Kingdom, pp. 25-32 (2021).
<https://doi.org/10.1109/PowerMEMS54003.2021.9658386>.
- [7] Liu, M., Qian, F., Mi, J. et al. “Dynamic interaction of energy-harvesting backpack and the

human body to improve walking comfort”, *Mech. Syst. Signal Process.*, **174**(1), pp. 101-109 (2022).

<https://doi.org/10.1016/j.ymssp.2022.109101>.

[8] Sharghi, H. and Bilgen O. “Energy Harvesting from Human Walking Motion using Pendulum-based Electromagnetic Generators”, *J. Sound Vib.*, **534** (3), pp. 117-123 (2022).

<https://doi.org/10.1016/j.jsv.2022.117036>.

[9] Huang, G., Lin, S. and Xie, L. “Human-in-the-loop optimization of knee-joint biomechanical energy harvester to maximize power generation with minimal user effort”, *Energy Conv. Manag.*, **283** (1), pp. 116-129 (2023).

<https://doi.org/10.1016/j.enconman.2023.116913>.

[10] Saha, C.R., O’donnell, T., Wang, N. et al. “Electromagnetic generator for harvesting energy from human motion”, *Sensor Actuat A-Phys*, **147**(1), pp. 248–253 (2008).

<https://doi.org/10.1016/j.sna.2008.03.008>.

[11] Liu, S., Li, H., Yeo, J.C.C. et al. “Solvent-optimized monolithic SWCNT-based thermoelectric generator for efficient electricity harvesting from body heat and sunlight”, *Carbon*, **203** (1), pp. 111-119 (2023).

<https://doi.org/10.1016/j.carbon.2022.11.057>.

[12] Lay-Ekuakille, A., Vendramin, G., Trotta, A. et al. “Thermoelectric generator design based on power from body heat for biomedical autonomous devices”, *2009 IEEE international workshop on medical measurements and applications*, Cetraro, Italy, pp. 1–4 (2009).

<https://doi.org/10.1109/MEMEA.2009.5167942>.

[13] Goll, E., Zenner, H. and Dalhoff, E. “Upper bounds for energy harvesting in the region of the human head”, *IEEE Trans. Biomed. Eng.*, **58**(11), pp. 3097–3103 (2011).

<https://doi.org/10.1109/TBME.2011.2163407>.

- [14] Delnavaz, A. and Voix, J. “Electromagnetic micro-power generator for energy harvesting from breathing”, *IECON 2012-38th Annual Conference on IEEE Industrial Electronics Society*, Montreal, Canada, pp. 984–988 (2012).
<https://doi.org/10.1109/IECON.2012.6388587>.
- [15] Abdelmageed, M.G., Fathelbab, A.M.R. and Abouelsoud, A.A. “Design and simulation of an energy harvester utilizes blood pressure variation inside superior vena cava”, *58th Annual Conference of the Society of Instrument and Control Engineers of Japan*, Hiroshima, Japan, pp. 1107 - 1112 (2019).
<https://doi.org/10.23919/SICE.2019.8859911>.
- [16] Zhang, Y., Lee, A. and Lee, C. “Design and application of piezoelectric and electromagnetic energy harvesters for mechanical energy harvesting in the human-body: A review”, *Sens. Actuators A: Phys.*, **370** (1), pp. 115-129 (2024).
<https://doi.org/10.1016/j.sna.2024.115207>.
- [17] Delnavaz, A. and Voix, J. “Piezo-magnetic energy harvesting from movement of the head”, *J. Phys. Conf. Ser.*, **660** (1), pp. 1-5 (2015).
<https://doi.org/10.1088/1742-6596/660/1/012120>.
- [18] Liu, M., Hughes-Oliver, C., Queen, R. et al. “Comparison of negative-muscle-work energy harvesters from the human ankle: Different designs and trade-offs”, *Renew. Energy*, **170** (2), pp. 525–538 (2021).
<https://doi.org/10.1016/j.renene.2021.01.151>.
- [19] Shepard, K., Ito, T. and Griffith, A.J. “Extracting energy from the inner ear”, *Nat. Biotechnol.*, **30**(12), pp.1204–1205 (2012).
<https://doi.org/10.1038/nbt.2448>.
- [20] Delnavaz, A. and Voix, J. “Energy harvesting for in-ear devices using ear canal dynamic motion”, *IEEE Trans. Ind. Electron.*, **61**(1), pp. 583–590 (2013).

<https://doi.org/10.1109/TIE.2013.2242656>.

[21] Wang, Y., Hong, M., Venezuela, J. et al. “Expedient secondary functions of flexible piezoelectrics for biomedical energy harvesting”, *Bioact. Mater.*, **22** (1), pp. 291-311 (2023).
<https://doi.org/10.1016/j.bioactmat.2022.10.003>.

[22] Qi, Y., Jafferis, N.T., Lyons Jr, K. et al. “Piezoelectric ribbons printed onto rubber for flexible energy conversion”, *Nano Lett.*, **10**(2), pp. 524–528 (2010).
<https://doi.org/10.1021/nl903377u>.

[23] Yang, R., Qin, Y., Dai, L. et al. “Power generation with laterally packaged piezoelectric fine wires”, *Nat. Nanotechnol.*, **4**(1), pp. 34–39 (2009).
<https://doi.org/10.1038/nnano.2008.314>.

[24] Cui, H., Hensleigh, R., Yao, D. et al. “Three-dimensional printing of piezoelectric materials with designed anisotropy and directional response”, *Nat. Mater.*, **18**(3), pp. 234–241 (2019).
<https://doi.org/10.1038/s41563-018-0268-1>.

[25] Delnavaz, A. and Voix, J. “Ear canal dynamic motion as a source of power for in-ear devices”, *J. Appl. Phys.*, **113**(6), pp. 64-71 (2013).
<https://doi.org/10.1063/1.4792307>.

[26] Delnavaz, A. and Voix, J. “Piezo-earpiece for micro-power generation from ear canal dynamic motion”, *J. Micromech. Microeng.*, **23**(11), pp. 114-121 (2013).
<https://doi.org/10.1088/0960-1317/23/11/114001>.

[27] Carioli, J., Delnavaz, A., Zednik, R.J. et al. “Power capacity from earcanal dynamic motion”, *AIP Adv.*, **6**(12), pp. 125-132 (2016).
<https://doi.org/10.1063/1.4971215>.

[28] Delnavaz, A. and Voix, J. “Flexible energy harvesting from hard piezoelectric beams”, *J.*

Phys. Conf. Ser., **773** (1), pp. 1-6 (2016).

<https://doi.org/10.1088/1742-6596/773/1/012065>.

[29] Carioli, J., Delnavaz, A., Zednik, R.J. et al. “Piezoelectric earcanal bending sensor”, *IEEE Sens. J.*, **18**(5), pp. 2060–2067 (2017).

<https://doi.org/10.1109/JSEN.2017.2783299>.

[30] Avetissian, T., Formosa, F., Badel, A. et al. “A novel piezoelectric energy harvester for earcanal dynamic motion exploitation using a bistable resonator cycled by coupled hydraulic valves made of collapsed flexible tubes”, *Micromachines*, **15**(3), pp. 1-27 (2024).

<https://doi.org/10.3390/mi15030415>.

[31] Stinson M.R. and Lawton B.W. “Specification of the geometry of the human ear canal for the prediction of sound-pressure level distribution”, *J. Acoust. Soc. Am.*, **85**(6), pp. 2492–2503 (1989).

<https://doi.org/10.1121/1.397744>.

[32] Egolf, D.P., Nelson, D.K., Howell III, H.C. et al. “Quantifying ear-canal geometry with multiple computer-assisted tomographic scans”, *J. Acoust. Soc. Am.*, **93**(5), pp. 2809–2819 (1993).

<https://doi.org/10.1121/1.405802>.

[33] Baer, T., Gore, J.C., Gracco, L.C. et al. “Analysis of vocal tract shape and dimensions using magnetic resonance imaging: Vowels”, *J. Acoust. Soc. Am.*, **90**(2), pp. 799–828 (1991).

<https://doi.org/10.1121/1.401949>.

[34] Darkner, S., Larsen, R. and Paulsen, R.R. “Analysis of deformation of the human ear and canal caused by mandibular movement”, *International Conference on Medical Image Computing and Computer-Assisted Intervention*, Morocco, Marrakesh, pp. 801–808 (2007).

https://doi.org/10.1007/978-3-540-75759-7_97.

[35] Griffin, M.F., Premakumar, Y., Seifalian, A.M. et al. “Biomechanical characterisation of the human auricular cartilages; implications for tissue engineering”, *Ann. Biomed. Eng.*, **44**(12), pp.

3460–3467 (2016).

<https://doi.org/10.1007/s10439-016-1688-1>.

[36] Chiu, L. L. Y., Giardini-Rosa, R., Weber, J.F. et al. “Comparisons of auricular cartilage tissues from different species”, *Ann. Otol. Rhinol. Laryngol.*, **126**(12), pp. 819–828 (2017).

<https://doi.org/10.1177/0003489417738789>.

[37] Maroudas, A., Muir, H. and Wingham, J. “The correlation of fixed negative charge with glycosaminoglycan content of human articular cartilage”, *Biochim. Biophys. Acta - Gen. Subj.*, **177**(3), pp. 492–500 (1969).

[https://doi.org/10.1016/0304-4165\(69\)90311-0](https://doi.org/10.1016/0304-4165(69)90311-0).

[38] Rho, J. Y., Ashman, R.B. and Turner, C.H. “Young’s modulus of trabecular and cortical bone material: ultrasonic and microtensile measurements”, *J. Biomech.*, **26**(2), pp. 111–119 (1993).

[https://doi.org/10.1016/0021-9290\(93\)90042-d](https://doi.org/10.1016/0021-9290(93)90042-d).

[39] Wang, D. and Ko, H. “Piezoelectric energy harvesting from flow-induced vibration”, *J. Micromech. Microeng.*, **20**(2), pp. 250-269 (2010).

<https://doi.org/10.1088/0960-1317/20/2/025019>.

[40] Shacham, S., Castel, D. and Gefen, A. “Measurements of the Static Friction Coefficient Between Bone and Muscle Tissues”, *J. Biomech. Eng.*, **132**(8), pp. 84-97 (2010).

<https://doi.org/10.1115/1.4001893>.

[41] Chen, D., Yi, S., Wu, W. et al. “Synthesis and characterization of novel room temperature vulcanized (rtv) silicone rubbers using vinyl-poss derivatives as cross linking agents”, *Polymer*, **51**(17), pp. 3867–3878 (2010).

<https://doi.org/10.1016/j.polymer.2010.06.028>.

[42] Song, H., Yang, S., Sun, S. et al. “Effect of miscibility and crystallization on the mechanical properties and transparency of pvdf/pmma blends”, *Polym-Plast Technol*, **52**(3), pp. 221–227

(2013).

<https://doi.org/10.1080/03602559.2012.735314>.

[43] Vaidyanathan, P.P. *Signals, Systems, and Signal Processing*, 1st Edn., Cambridge University Press, Cambridge, UK, 2024.

List of figure captions

Figure 1: Fabricated ear mold in open mouth position.

Figure 2: CT-Scan images of the ear canal cross sections: (a) Axial plane, (b) Sagittal plane and (c) Coronal plane.

Figure 3: The workflow for generating the ear canal geometry with different parts, (1) soft tissue, (2) earmold, (3) part of temporal and (4) condyle of mandible: (a) Model in Mimix, (b) Model in 3matic, (c) Model in Catia

Figure 4: Model of the plugin with piezoelectric layer.

Figure 5: Capturing mandible motion during speaking by opti-track camera: (a) connected markers, (b) opti-track camera.

Figure 6: Mouth closing percent during: (a) Discussion, (b) Text reading, (c) Poem reading, (d) Greeting and (e) Loudly speaking.

Figure 7: The schematic model of the ear canal and ear mold.

Figure 8: Homonymous surfaces in contact with each other: (a,b) Soft tissue inner surface, (c) Soft tissue outer surface, (d) Condyle of mandible outer surface, (e,f) Temporal outer surface and (g) Plugin.

Figure 9: Discretized model for finite element simulations.

Figure 10: Piezoelectric output voltage: (a) Discussion, (b) Text reading, (c) Poem reading, (d) Greeting and (e) Loudly speaking.

Figure 11: PVDF orientation: N: Normal to piezoelectric surface, L: Tangent to piezoelectric surface in Longitudinal direction and T: Tangent to piezoelectric surface in circumferential direction

Figure 12: Output voltage in different piezoelectric orientations: (a) normal direction, (b) tangential direction and (c) longitudinal direction.

Figure 13: The stress distribution in piezoelectric in close mouth position.

Figure 14: Piezoelectric strain with different cartilage stiffness: (a) $E=1.03$ Mpa, (b) $E=1.66$ Mpa, (c) $E=2.29$ Mpa

Figure 15: Output voltage in different cartilage stiffness.

Figure 16: Piezoelectric strain with different earmold stiffness: (a) $E=1.66$ Mpa, (b) $E=1.25$ Mpa, (c) $E=0.83$ Mpa.

Figure 17: Output voltage in different ear mold stiffness.

Figure 18: Piezoelectric strain with different coefficient of friction between condyle of the mandible and soft tissue: (a) Maximum friction coefficient, (b) Average friction coefficient, (c) Minimum friction coefficient.

Figure 19: Output voltage with different coefficient of friction between condyle of the mandible and soft tissue.

Figure 20: Piezoelectric actual output voltage during: (a) Discussion, (b) Text reading, (c) Poem reading, (d) Greeting and (e) Loudly speaking.

Figure 21: Current rectifier circuit: (a) Schematic and (b) Simulation in Matlab Simulink.

List of table captions

Table 1: Cartilage and earmold mechanical properties [35-37]

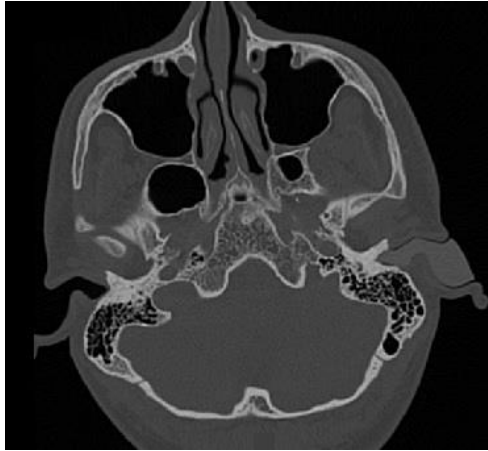
Table 2: Mechanical properties of the RTV silicone rubber [41]

Table 3: Time intervals of talking types considered in the simulation

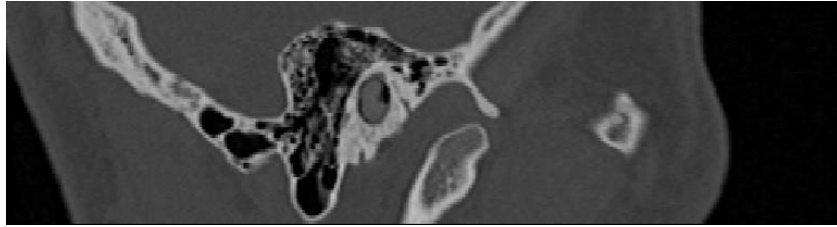
Figures:



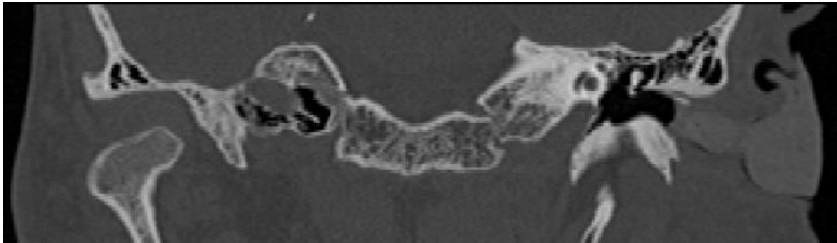
Figure 1



(a)

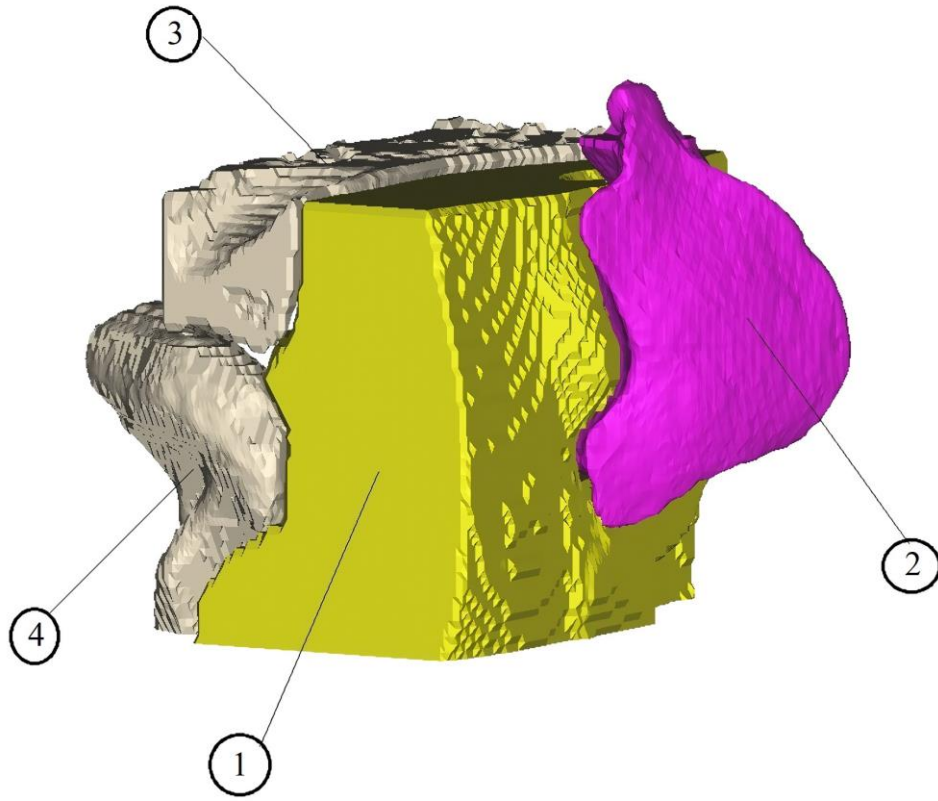


(b)

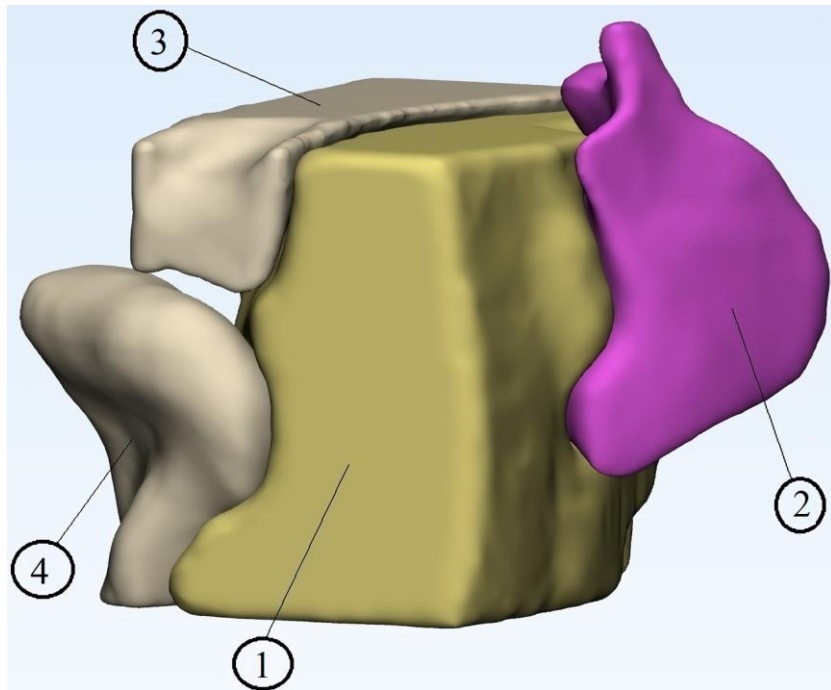


(c)

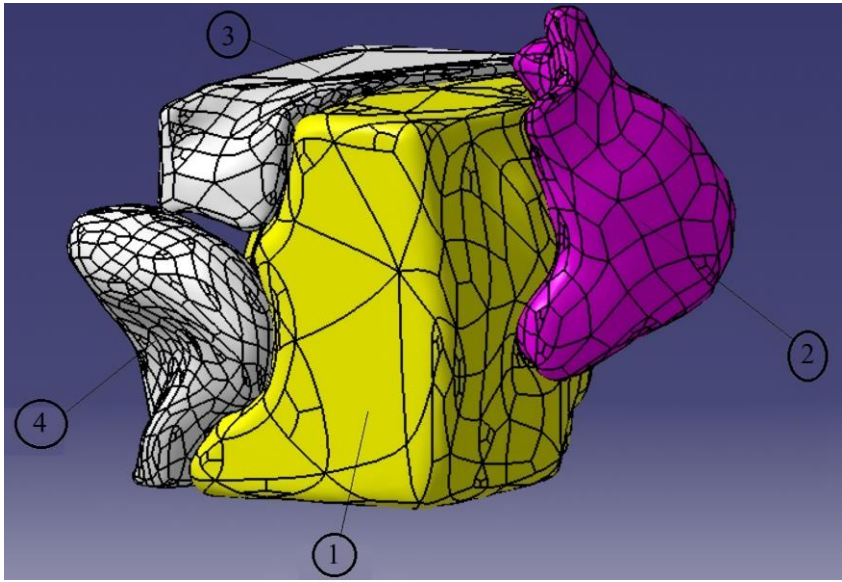
Figure 2



(a)



(b)



(c)

Figure 3

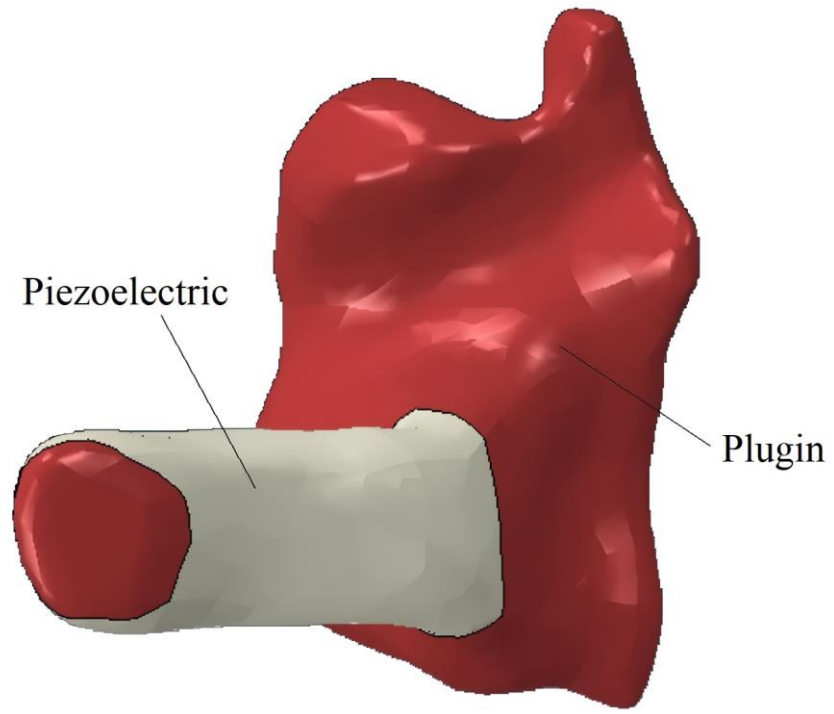


Figure 4

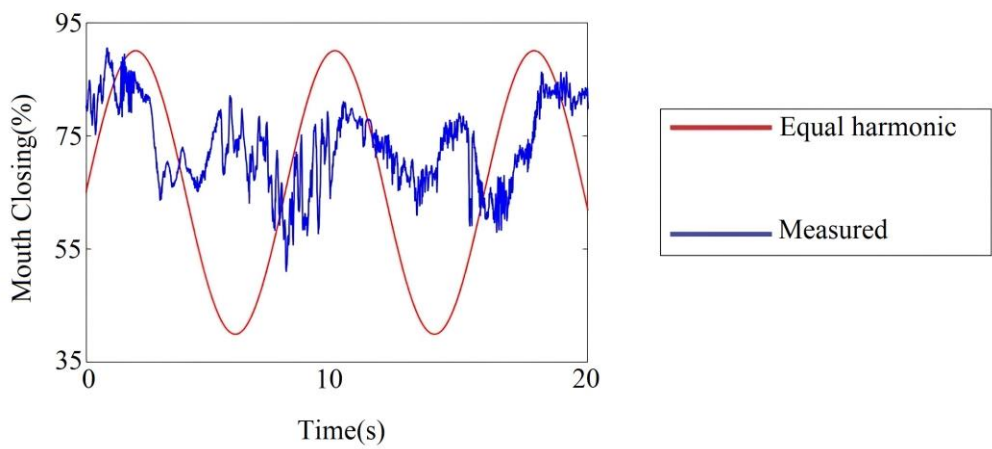


(a)

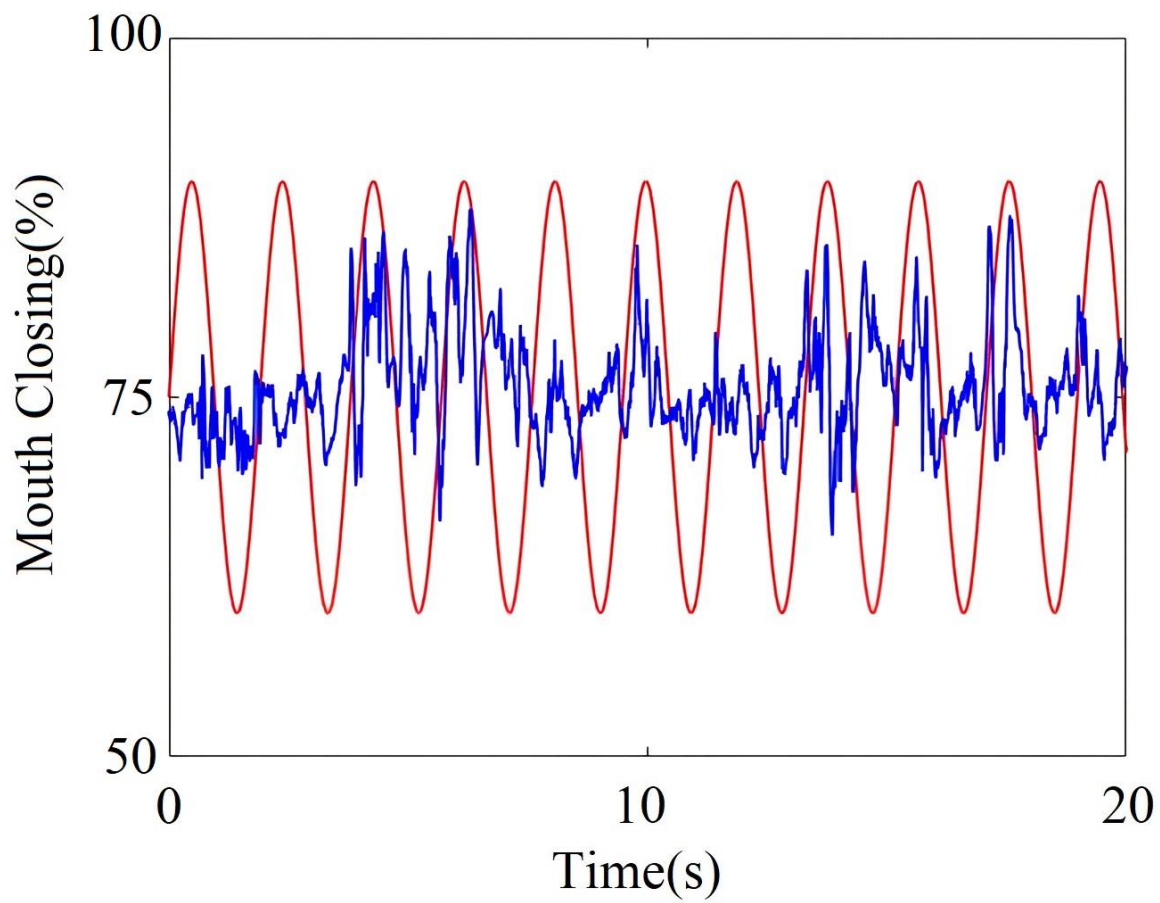


(b)

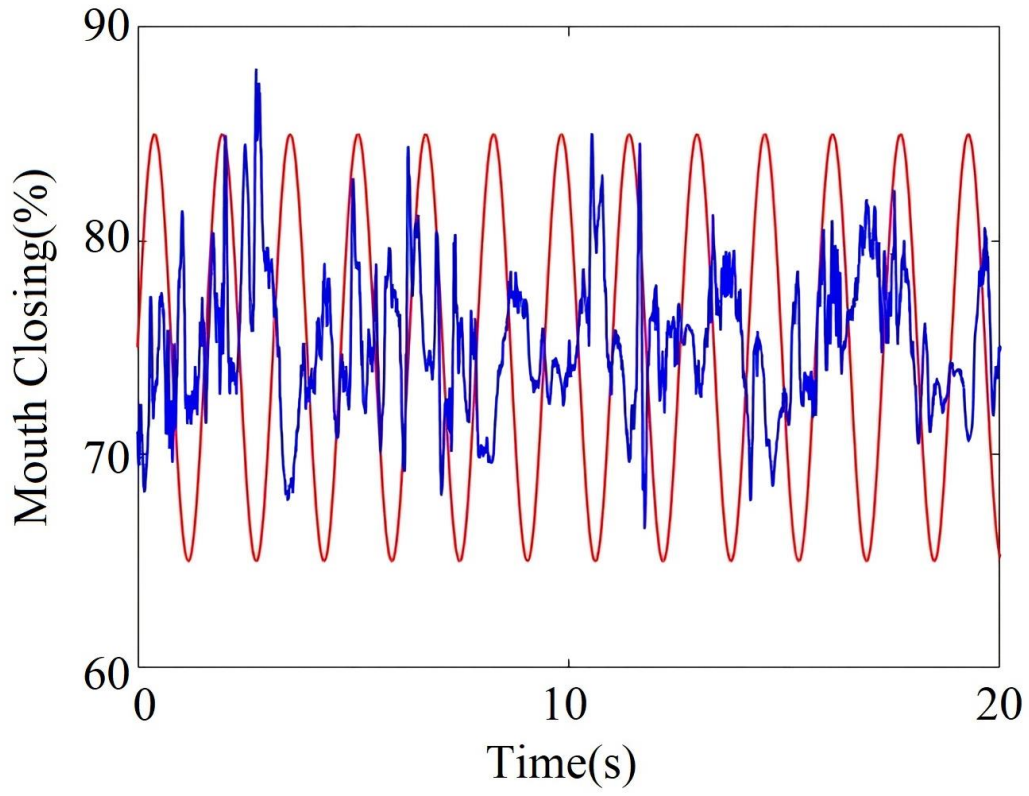
Figure 5



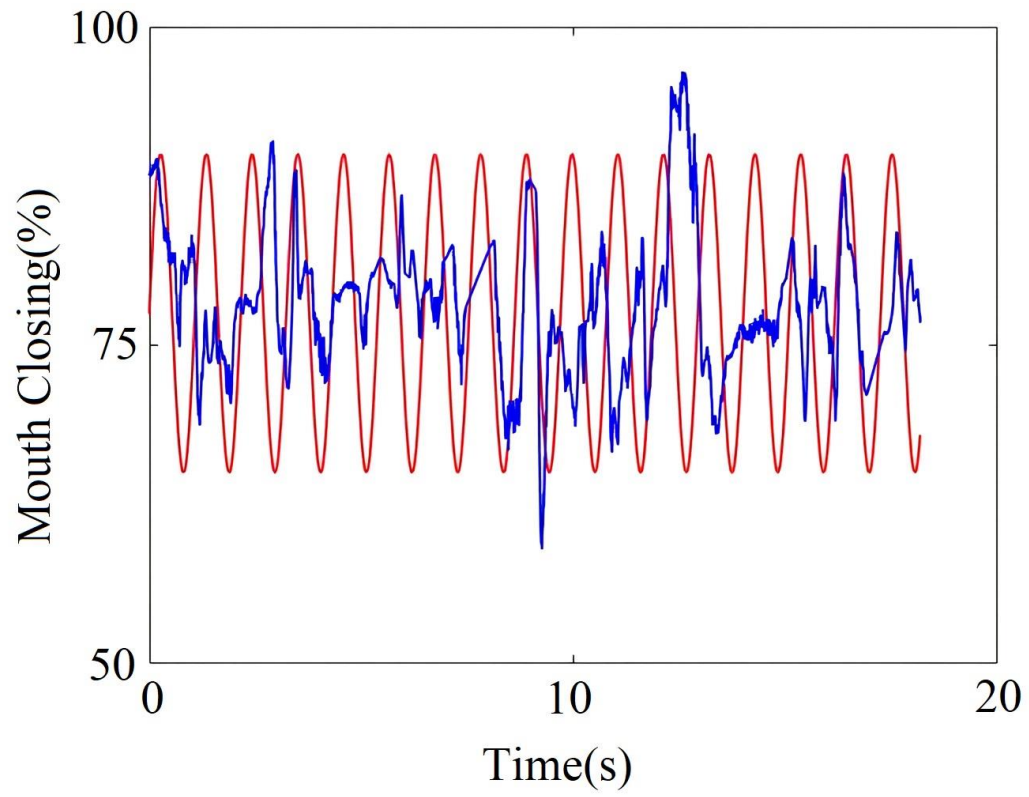
(a)



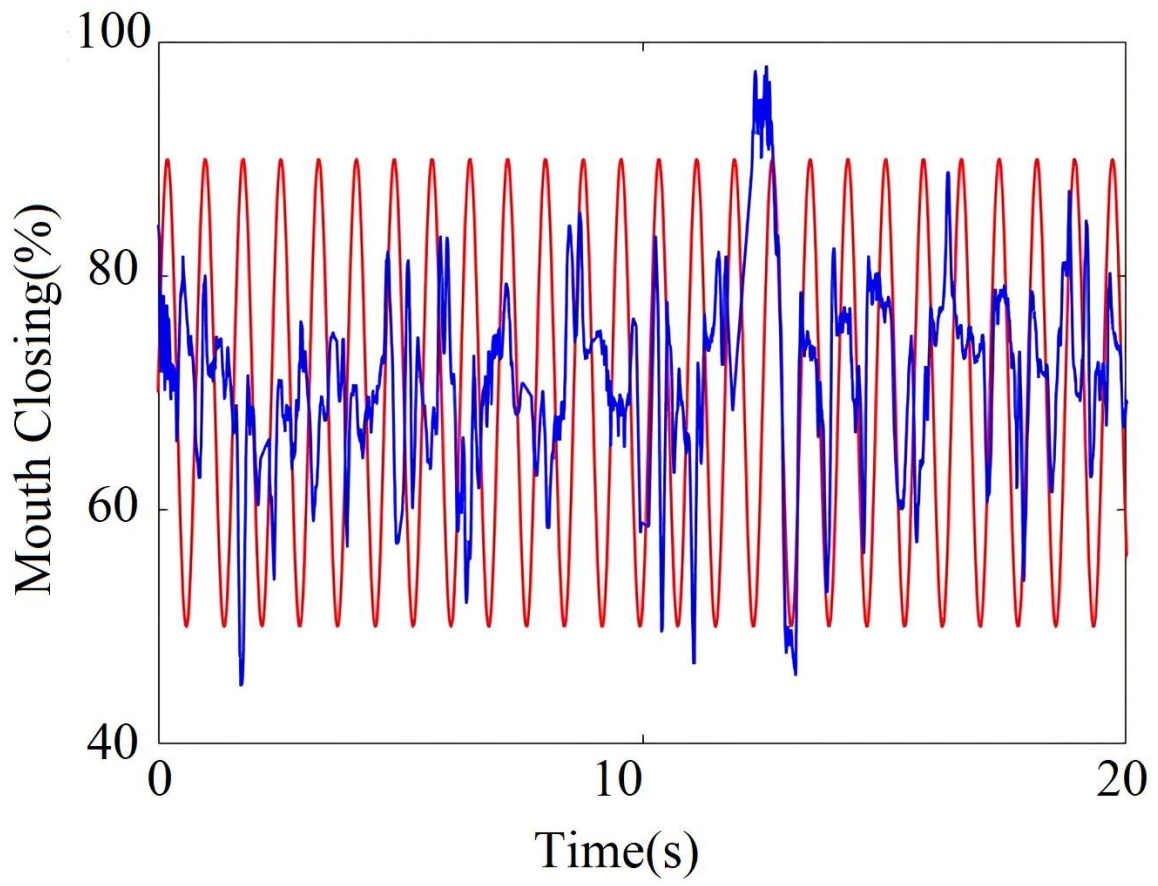
(b)



(c)



(d)



(e)

Figure 6

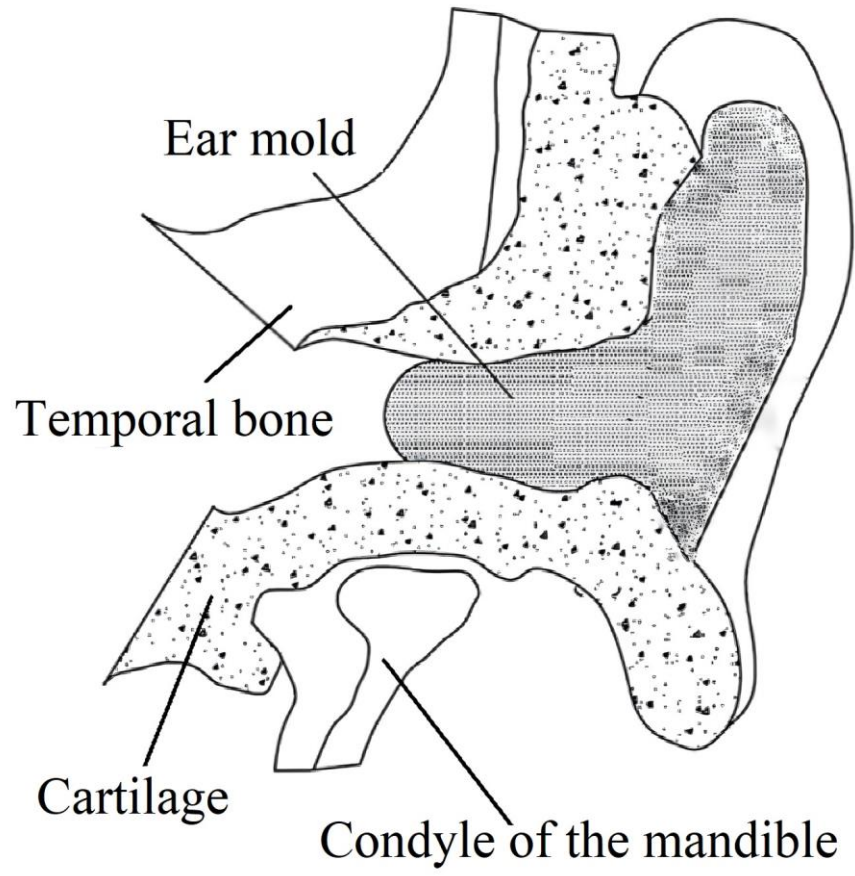


Figure 7

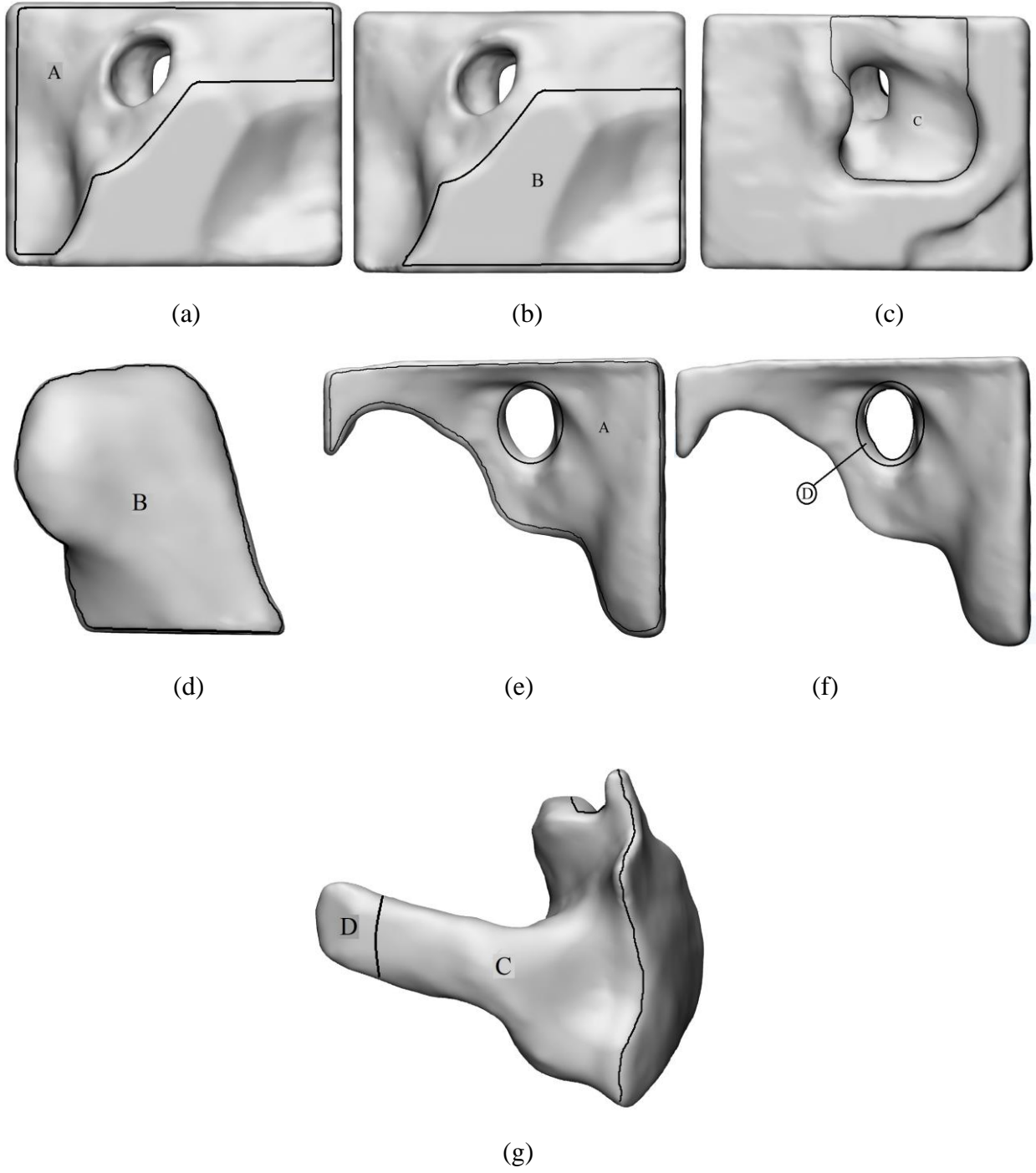


Figure 8

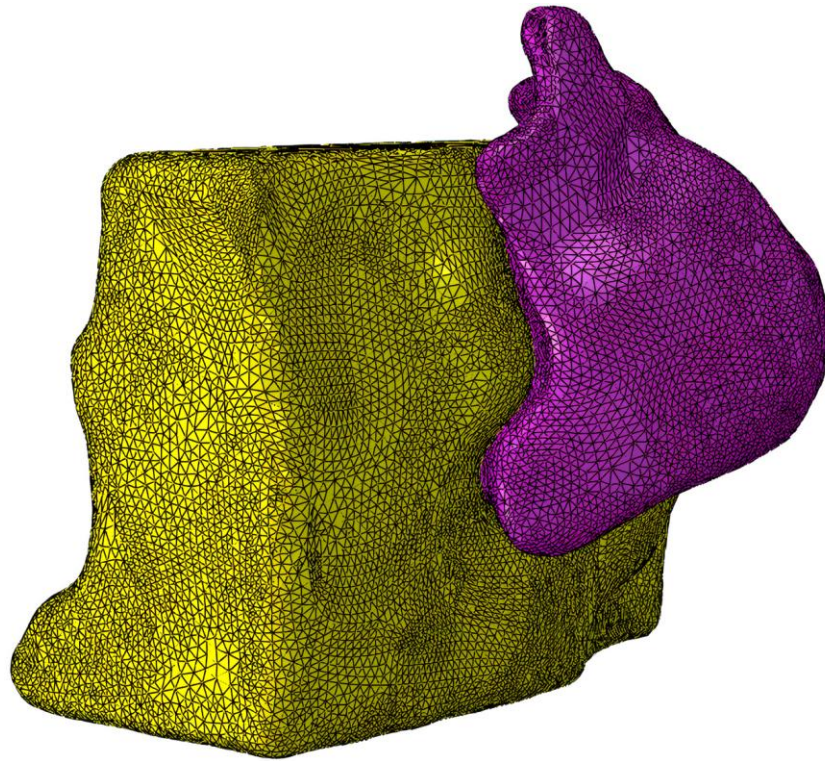
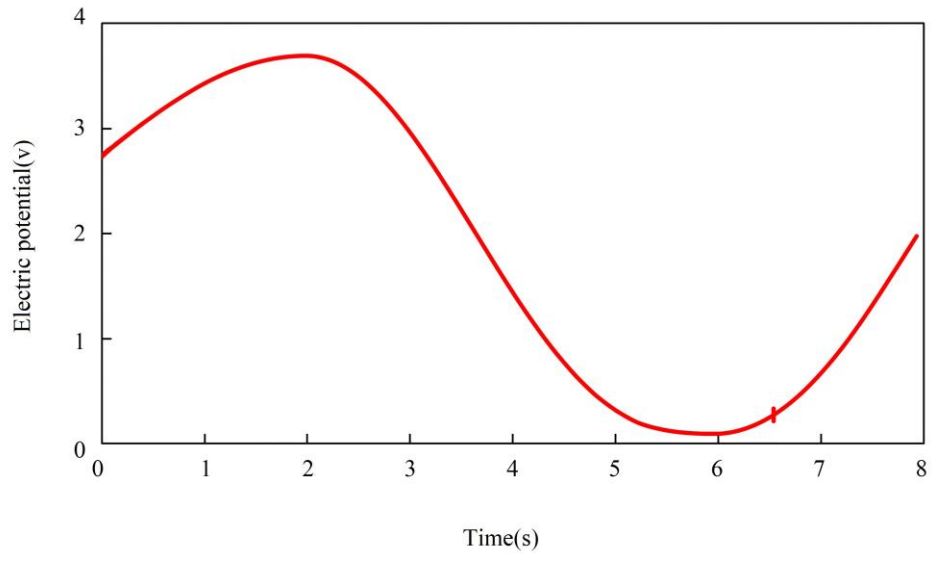
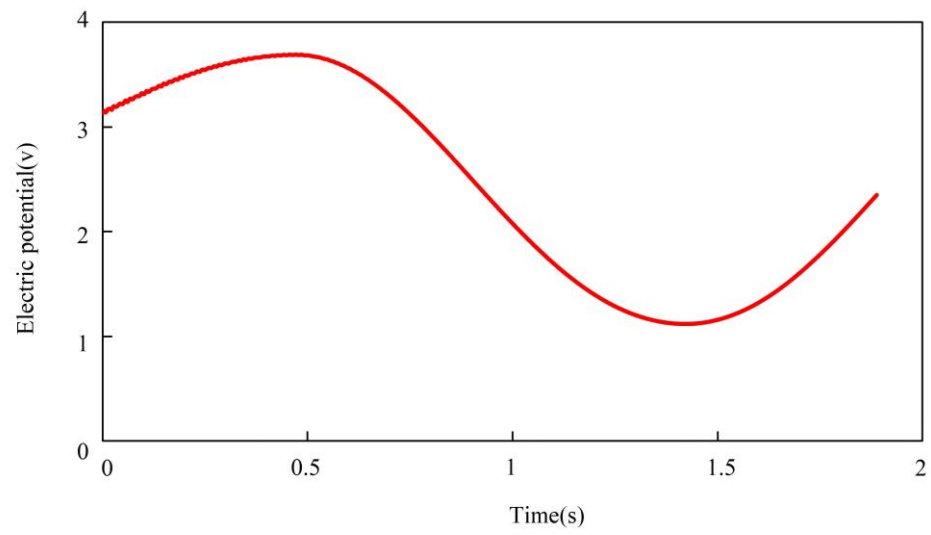


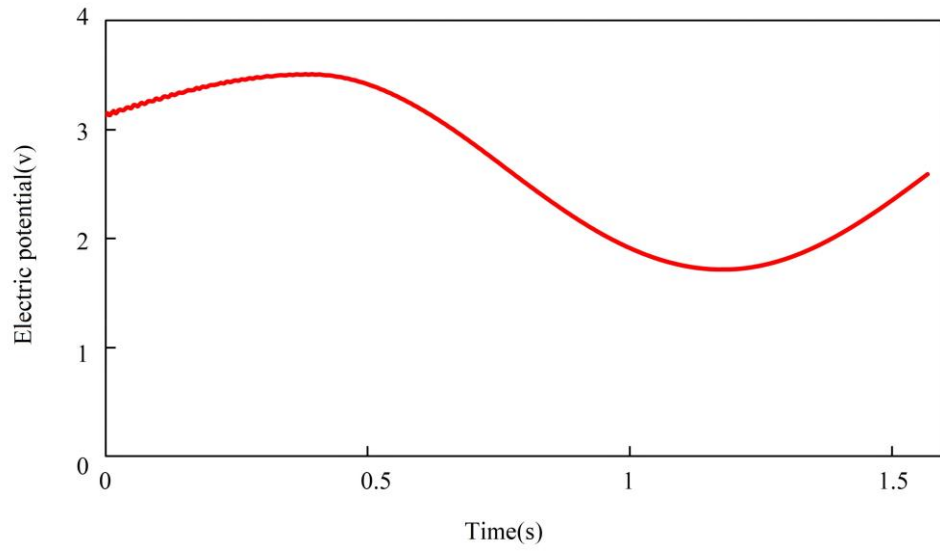
Figure 9



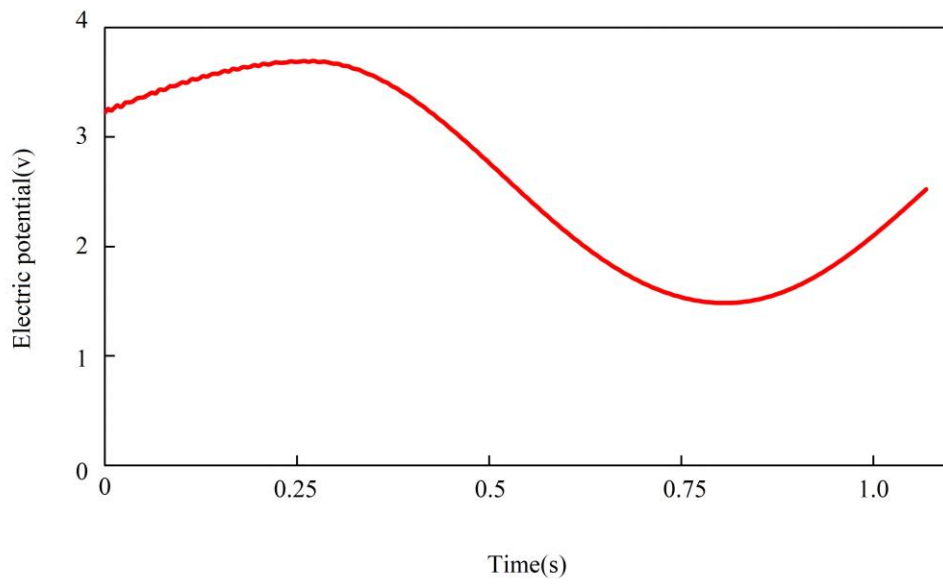
(a)



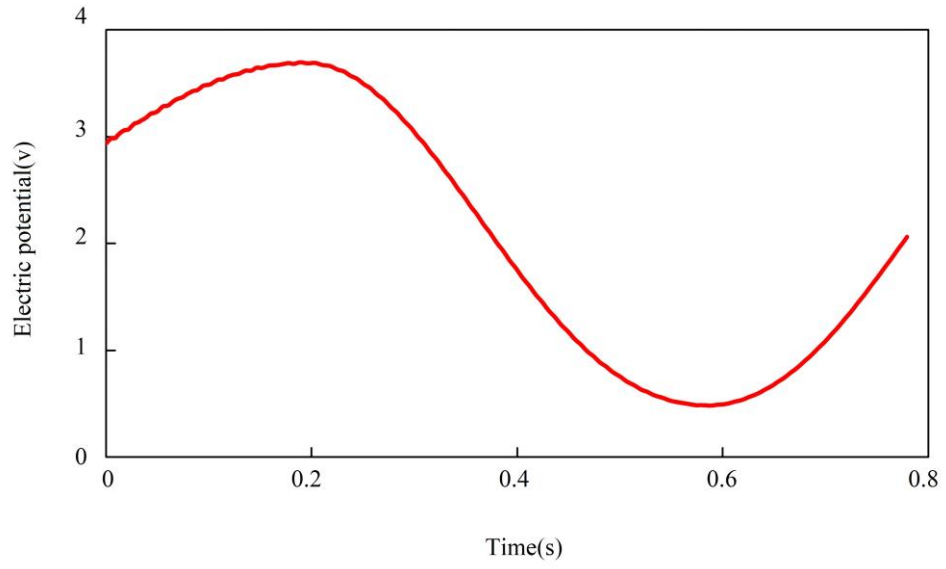
(b)



(c)



(d)



(e)

Figure 10

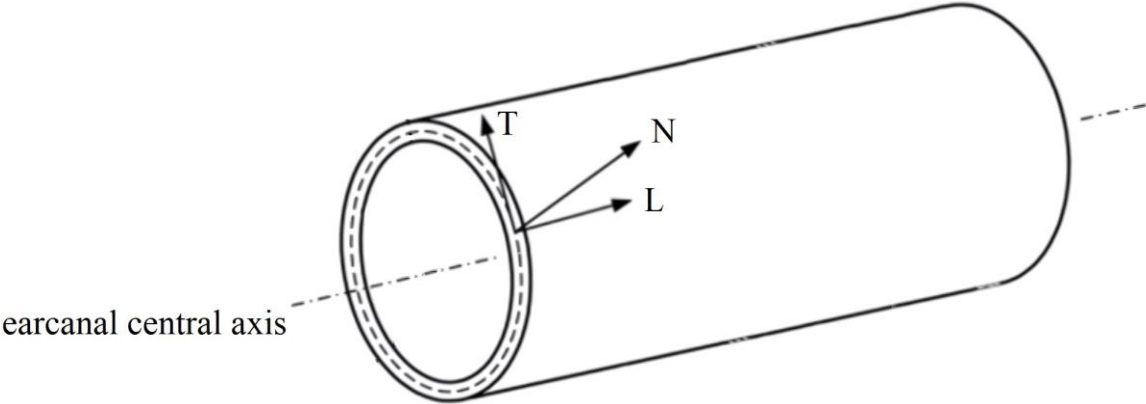
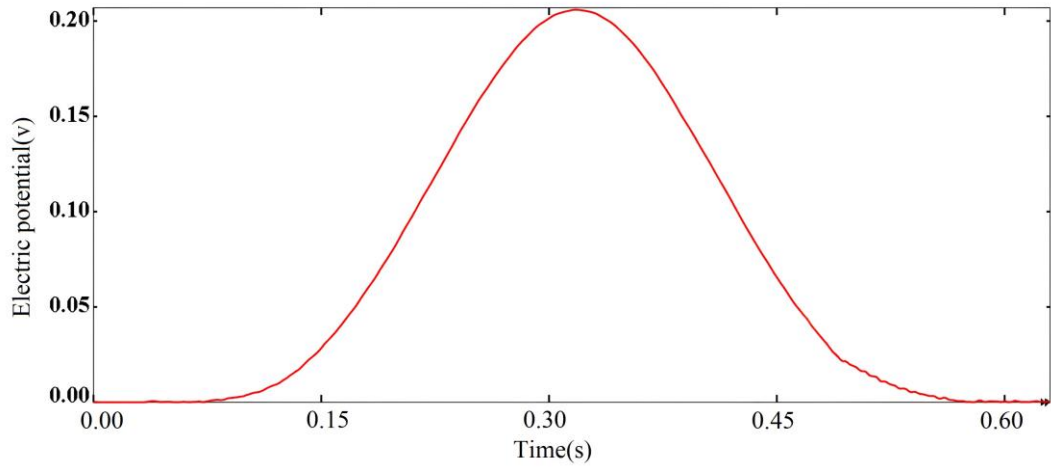
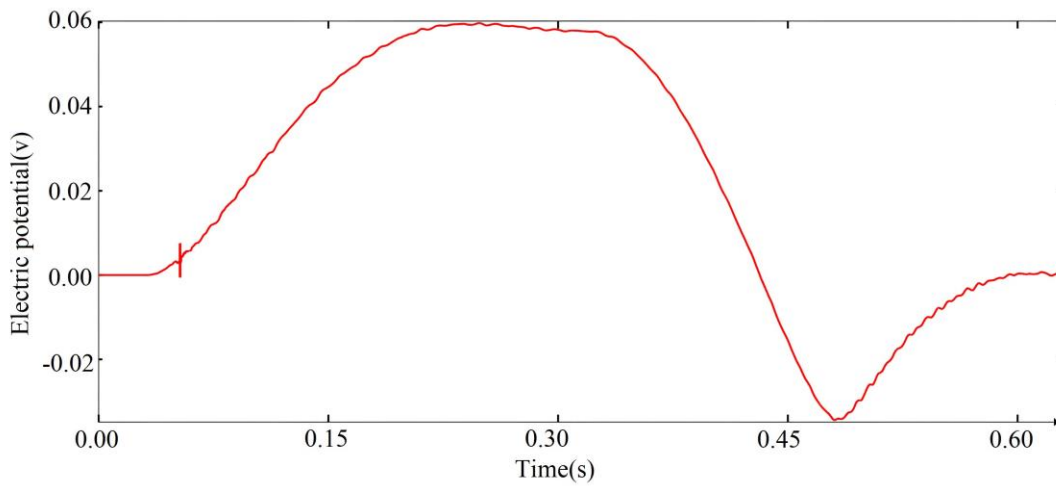


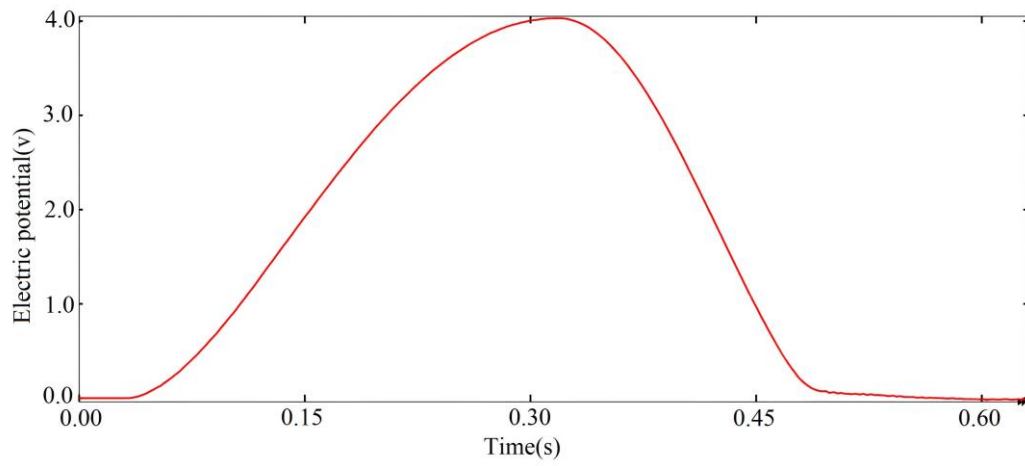
Figure 11



(a)



(b)



(c)

Figure 12

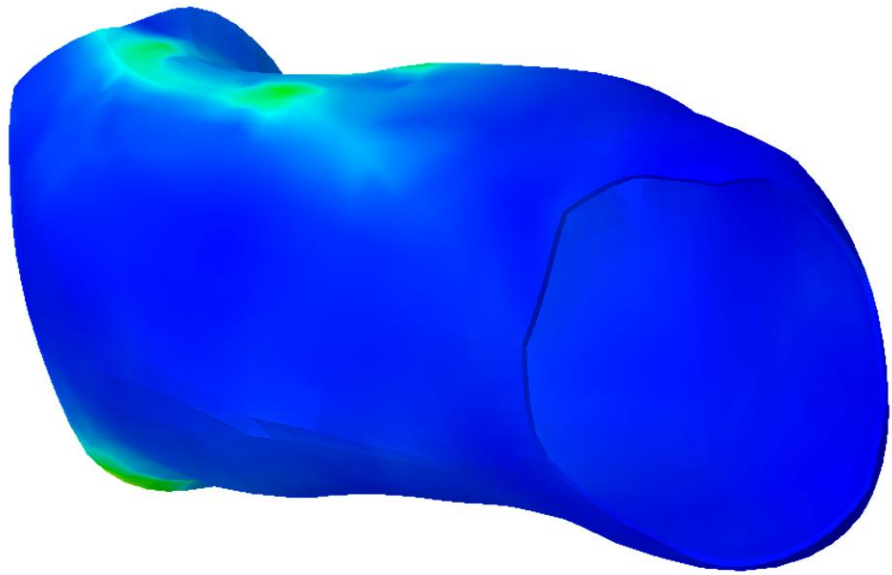
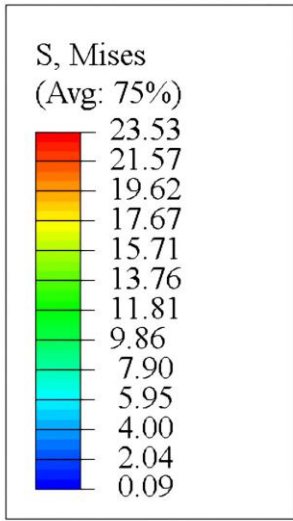
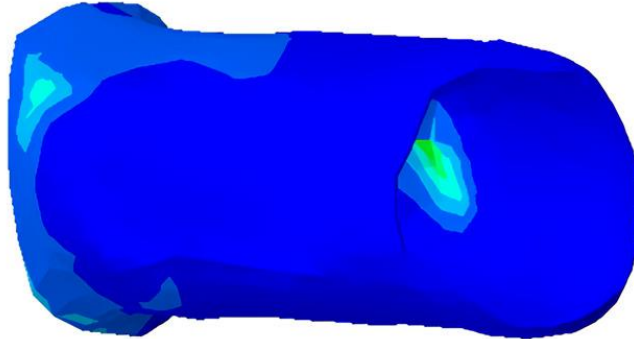
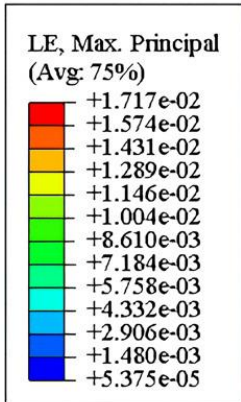
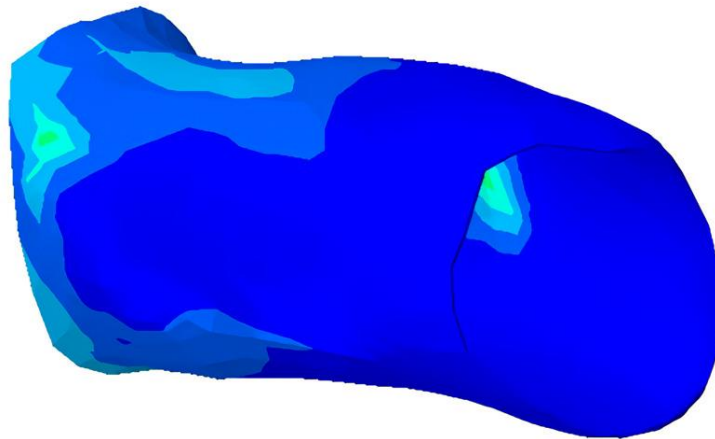
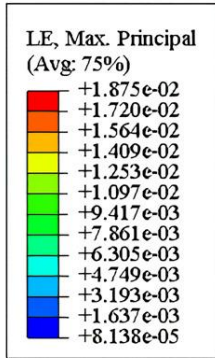


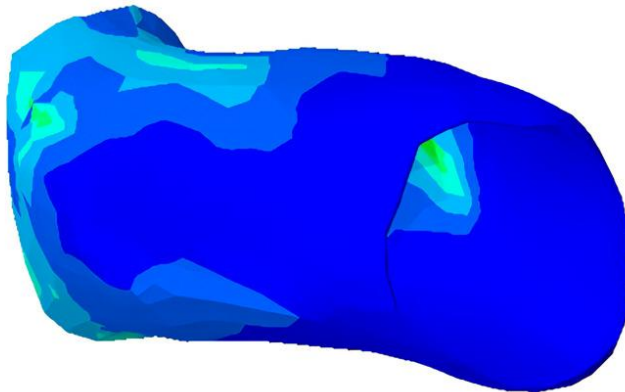
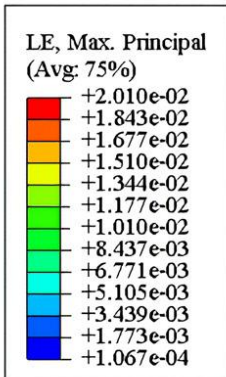
Figure 13



(a)



(b)



(c)

Figure 14

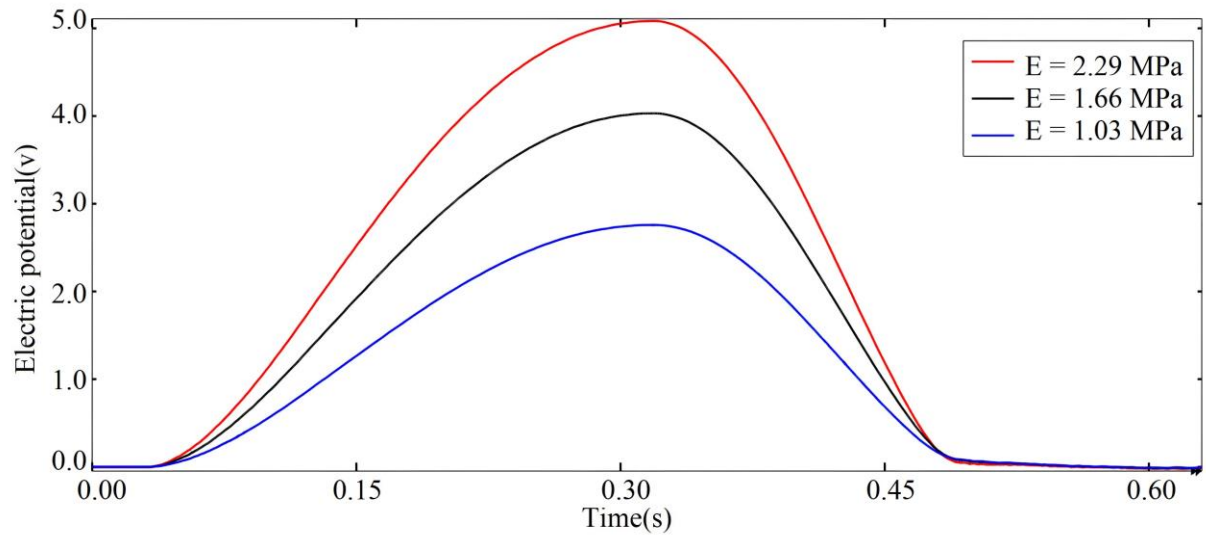
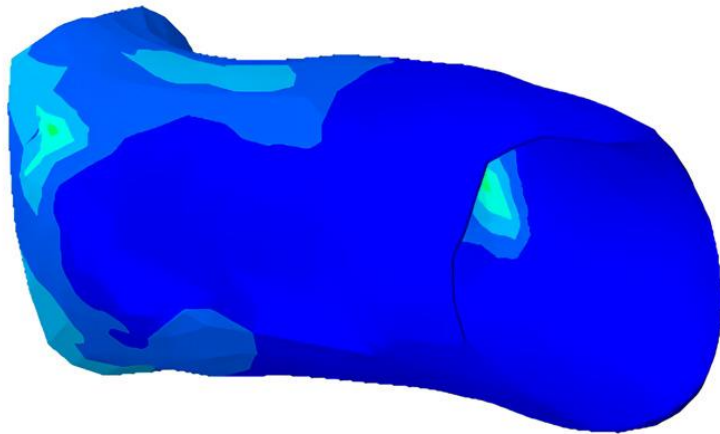
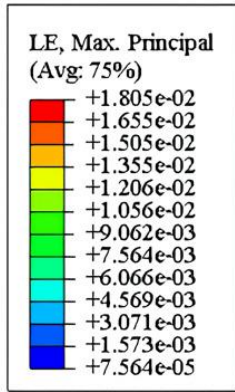
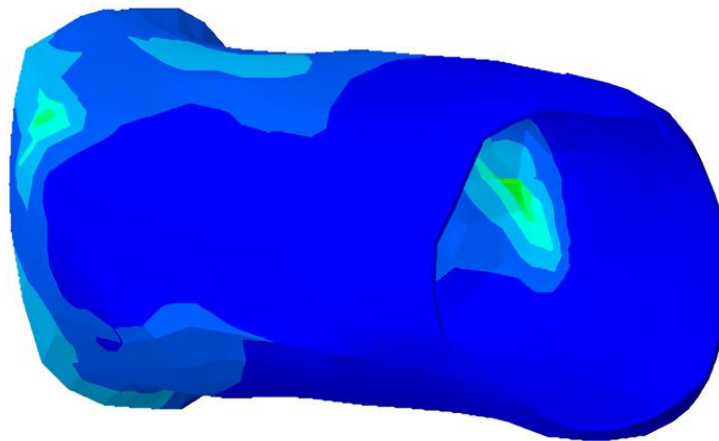
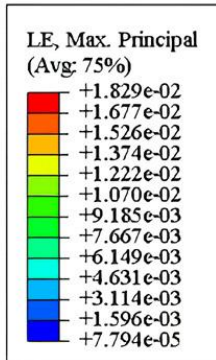


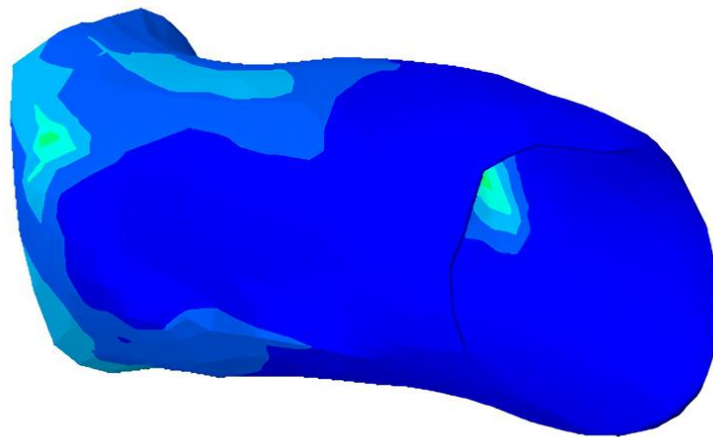
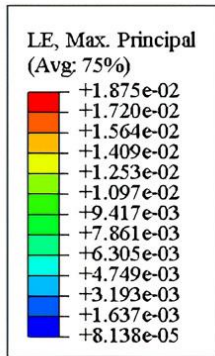
Figure 15: Output voltage in different cartilage stiffness.



(a)



(b)



(c)

Figure 16

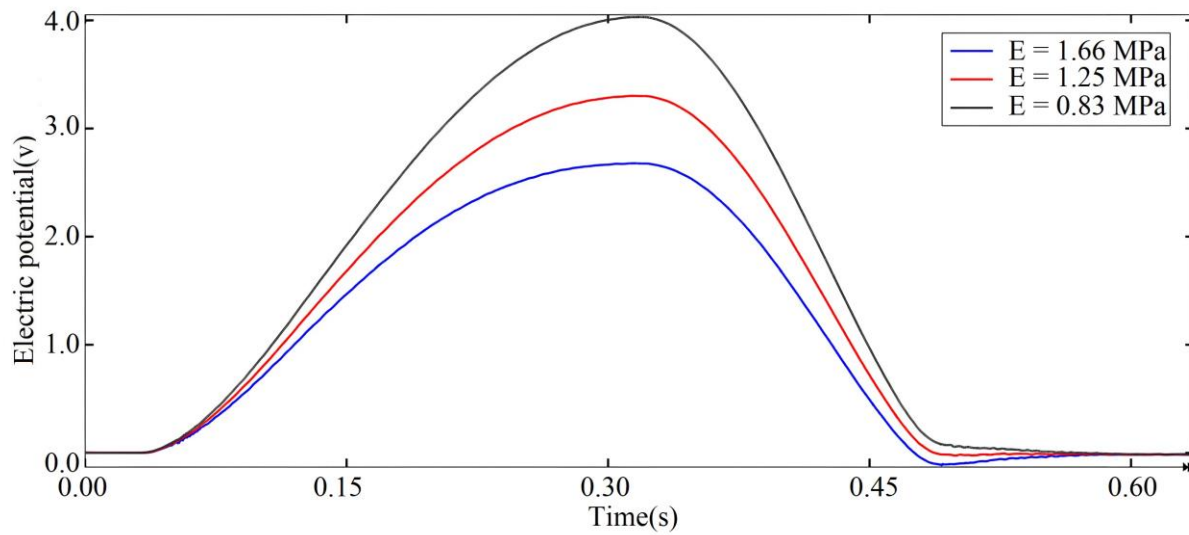
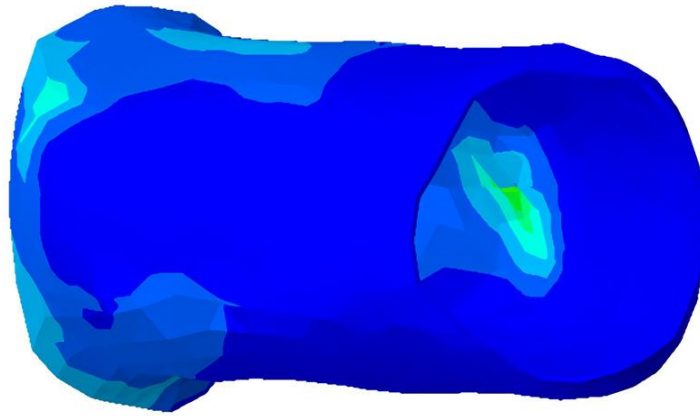
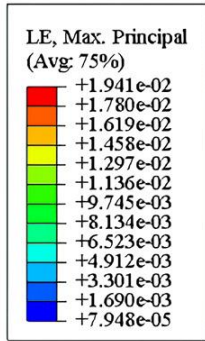
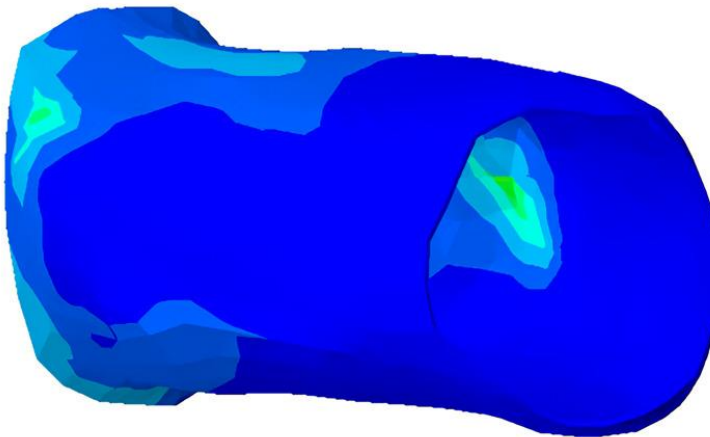
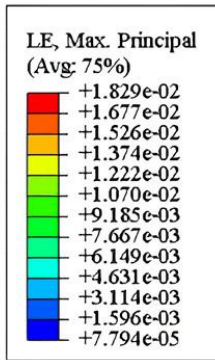


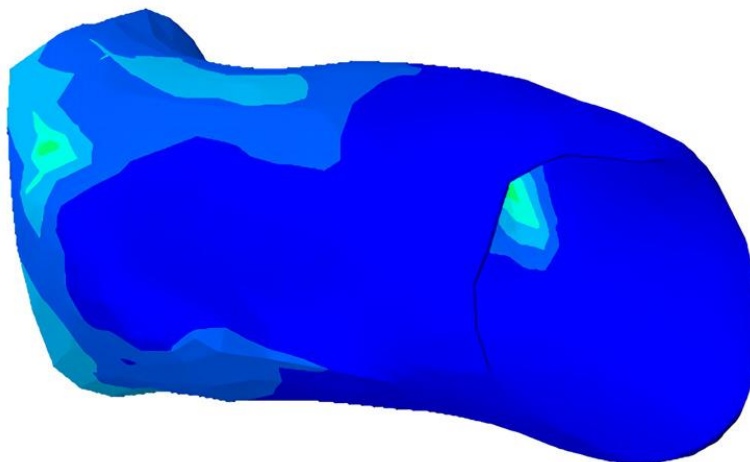
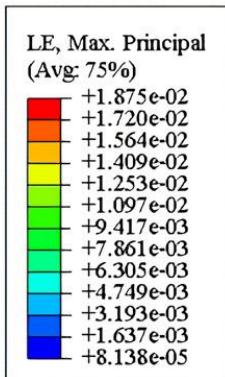
Figure 17: Output voltage in different ear mold stiffness.



(a)



(b)



(c)

Figure 18

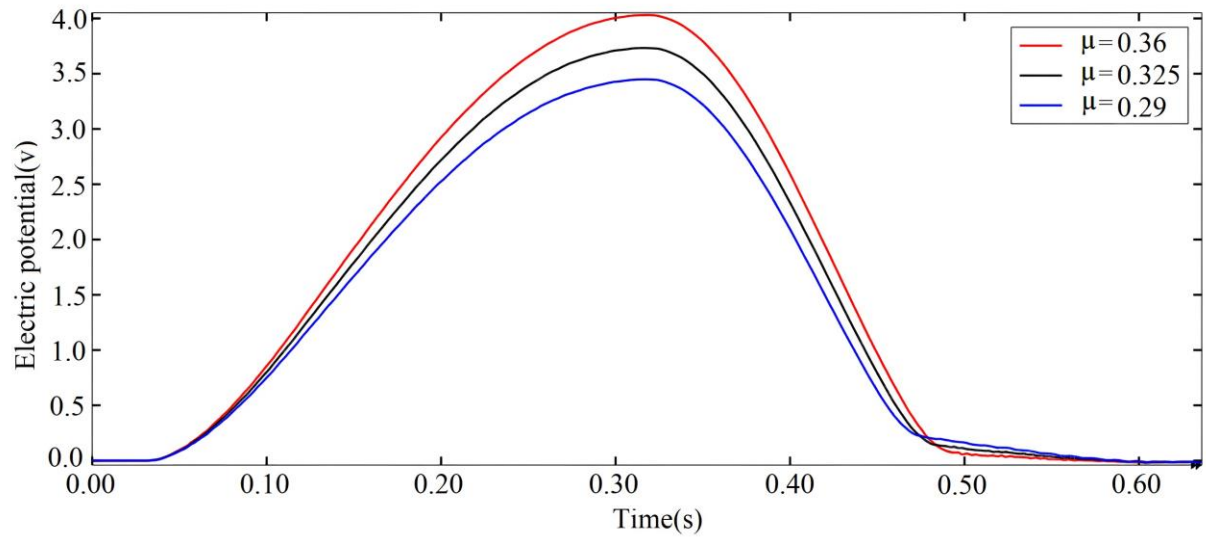
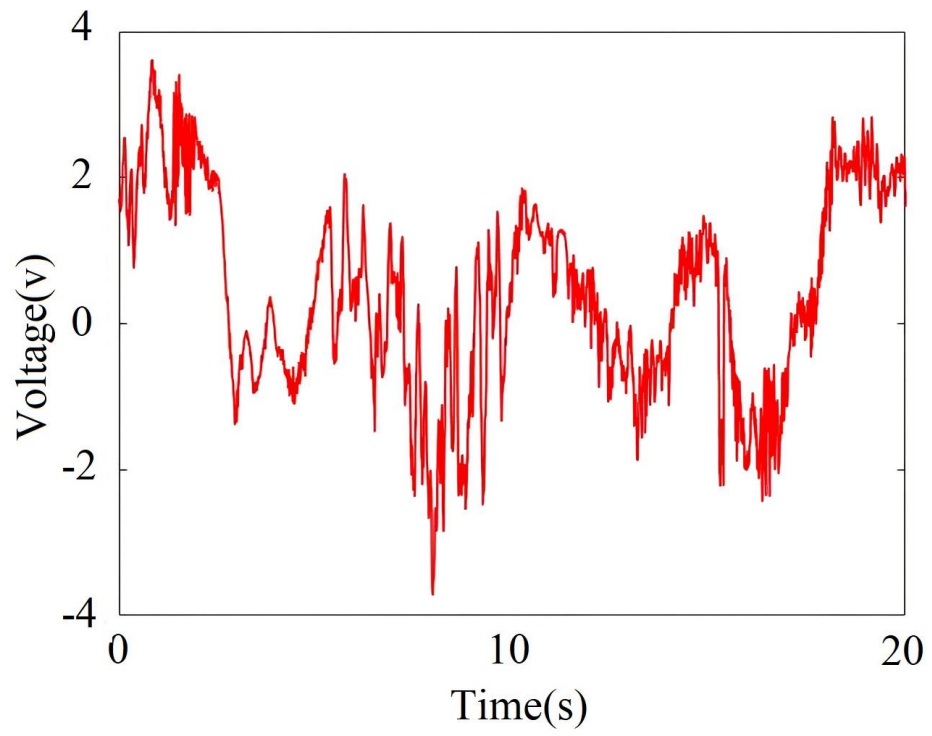
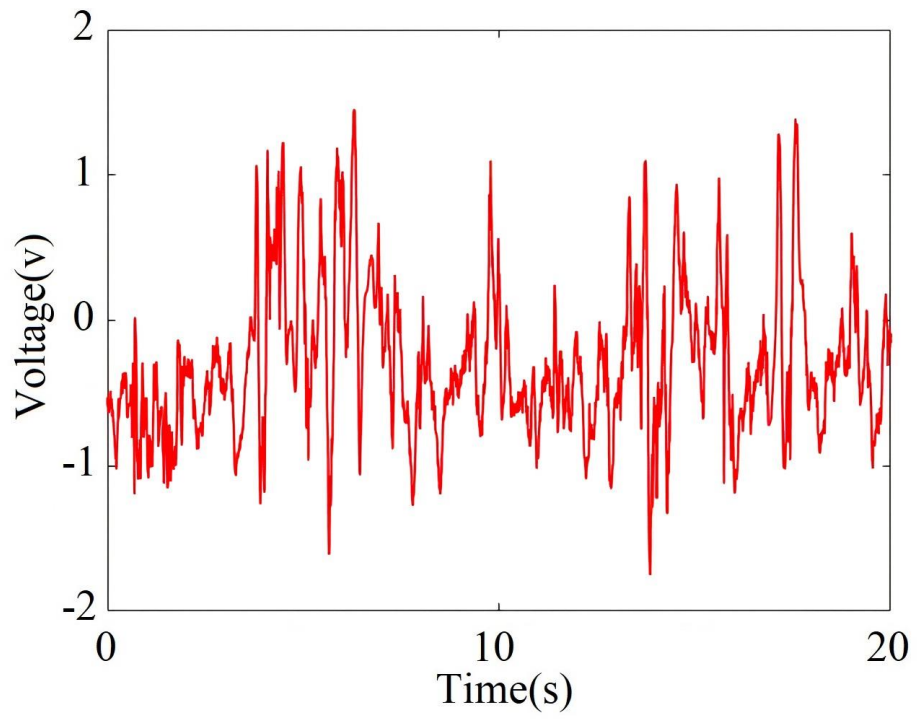


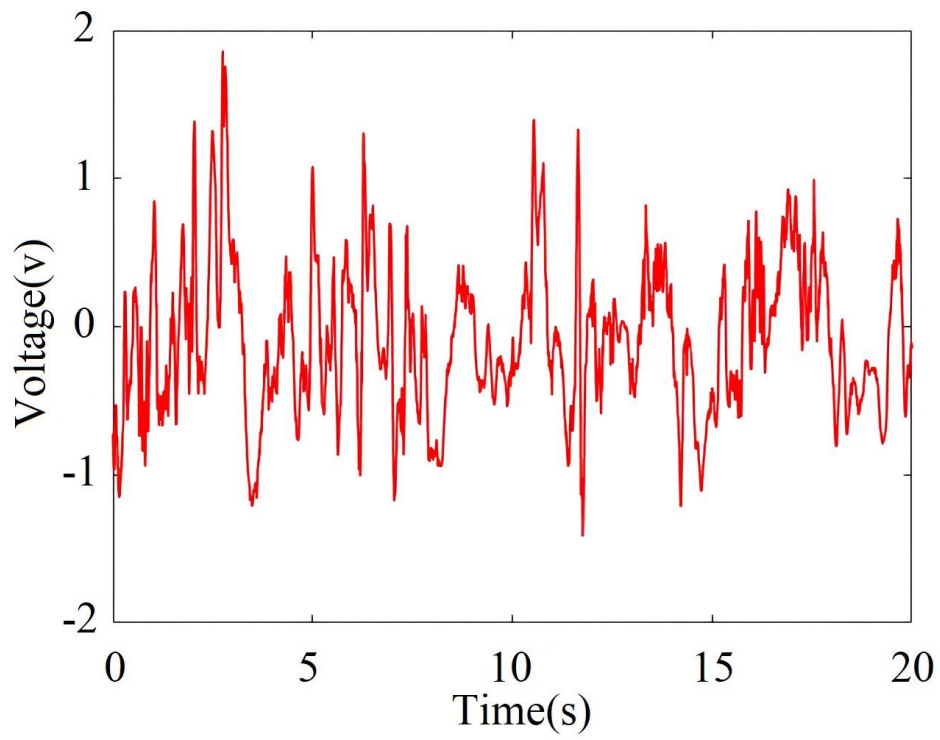
Figure 19



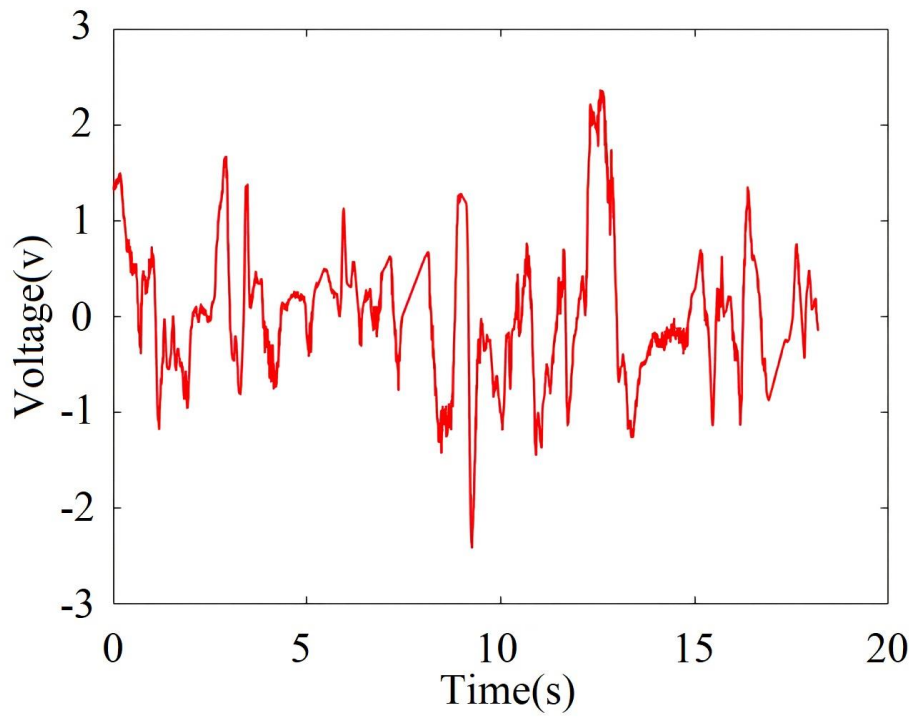
(a)



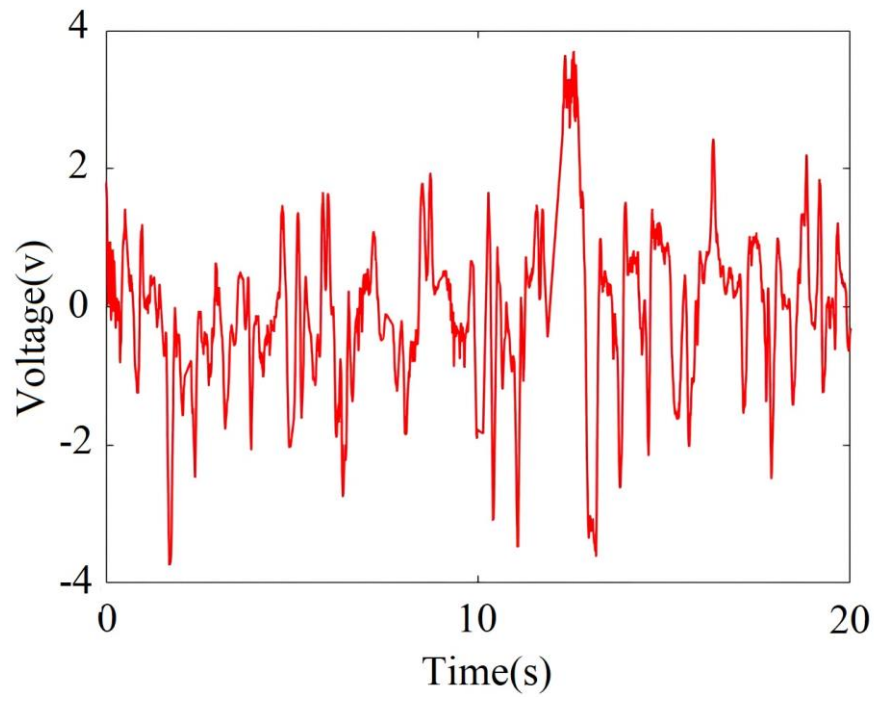
(b)



(c)

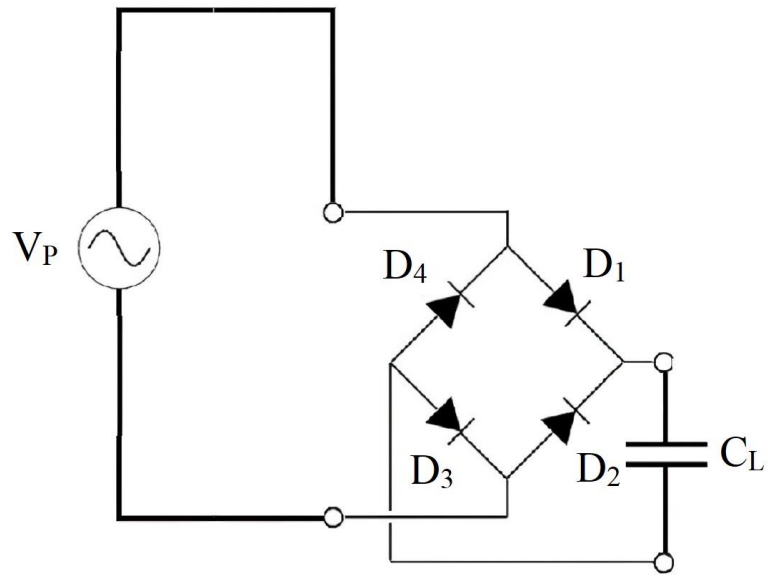


(d)

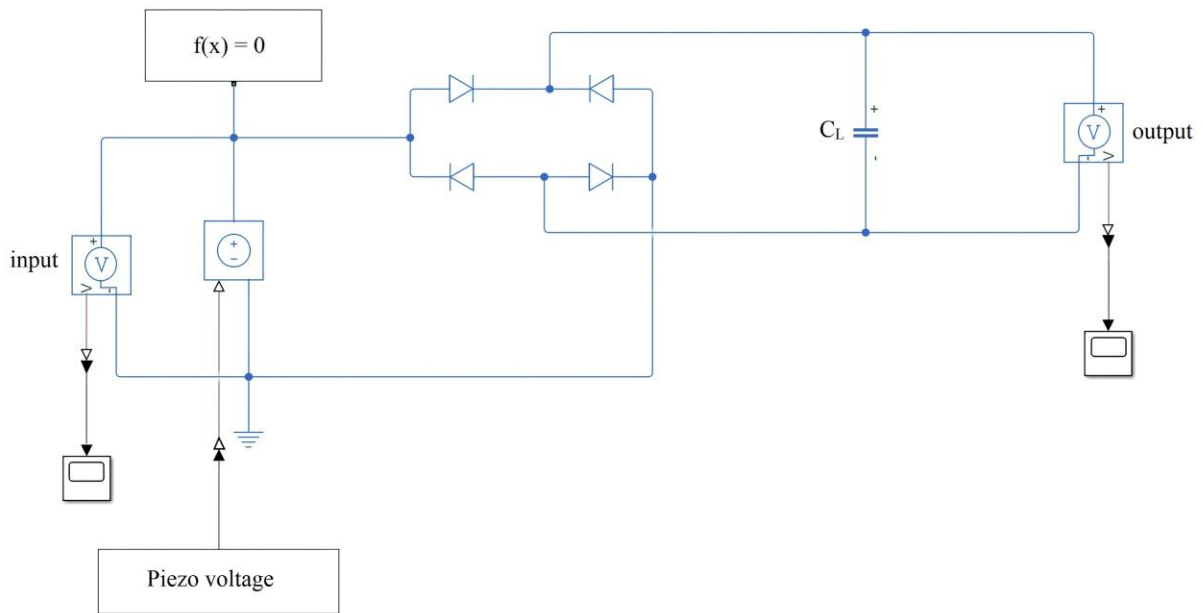


(e)

Figure 20



(a)



(b)

Figure 21

Tables

Table 1

Cartilage		
Young's modulus (MPa)	Poisson's ratio	Density ($\frac{kg}{m^3}$)
1.66±0.63	0.2	1080±10
Earmold		
0.83	0.47	1100

Table 2

Sample	Tensile strength (MPa)	Modulus (MPa)
TM-1	0.5	0.430
TE-1	0.469	0.315
OP-1	0.914	0.413
DVP-1	0.559	0.385
TE-2	0.514	0.347
OP-2	1.050	0.451
DVP-2	1.105	0.454

Table 3

Talking type	Time (min)	Generated energy (mJ)
Greeting	15	3.5
Talking aloud	5	0.825
Reading poetry	10	0.96
Reading text	30	0.306
Discussion	120	8.2
Total	180	13.8

Biography

Mohammadreza Salemi: received the B.Sc. degree in mechanical engineering from Yazd University, Yazd, Iran in 2020. During 2020–2022, he was M.Sc. student at the mechanical engineering department of Yazd University. His research interests are energy harvesting and smart materials.

Mohammad Mahdi Jalili: received the M.S. and the Ph.D. degrees in mechanical engineering from the Sharif University of Technology, Tehran, Iran, in 2003 and 2009, respectively. He is Associate Professor of Mechanical engineering at the Yazd University. His research interests include railway and road vehicles dynamics, vibration and acoustics and energy harvesting systems. He is author of more than 100 papers in international journals and refereed conferences.

Mohammad Jafari: received his B.S. and M.S. and Ph.D. degrees all in Mechanical Engineering from Isfahan University of Technology, Isfahan, Iran in 2011, 2013 and 2018, respectively. In 2021, he joined the Department of Mechanical Engineering, Yazd University, Yazd, Iran, where he is currently an assistant professor. His current research interests include computational mechanics, mechanics of materials, bio-inspired engineering, localization and failure mechanisms.

Mohammad Hadi Honarvar: received the B.Sc. and M.Sc. degrees in mechanical engineering and biomechanical engineering from the Sharif University of Technology, Tehran, Iran, in 2006 and 2009 respectively. He received Ph.D. degree in mechanical engineering from the Tokyo Institute of Technology in 2013. From 2015, he is assistant professor of mechanical engineering at Yazd University, Yazd, Iran. His current research interests include occupational biomechanics and optimization.